$[Cu_2(L\text{-}Et)(N_3)][BF_4]_2$, 79736-45-1; $[Cu_2(L\text{-}Et)(pyl)][ClO_4]_2$, 79736-48-4; $[Cu_2(L\text{-}Et)(NO_2)][ClO_4]_2$, 79736-50-8; $[Cu_2(L\text{-}Et)(HCOO)][ClO_4]_2$, 90991-19-8; 1,2-diaminobenzene, 95-54-5; 2-hydroxy-1,3-diaminopropanetetraacetic acid, 3148-72-9.

Supplementary Material Available: Atom numbering schemes (diagrams I and II) and tables of bond lengths (Tables A and B), bond angles (Tables C and D), and final atomic coordinates and thermal parameters (Tables E and F) for the acetate and azide complexes, respectively (19 pages). Ordering information is given on any current masthead page.

Thermal and Light-Induced Reduction of $Ru(bpy)_3^{3+}$ in Aqueous Solution

Pushpito K. Ghosh, Bruce S. Brunschwig, Mei Chou, Carol Creutz,* and Norman Sutin*

Contribution from the Department of Chemistry, Brookhaven National Laboratory, Upton, New York 11973. *Received August 22, 1983*

Abstract: The spontaneous reduction of $Ru(bpy)_3^{3+}$ to $Ru(bpy)_3^{2+}$ in aqueous solutions yields only trace O_2 and is accompanied by degradation of ~10% of the tris(bipyridine) complex. Carbon dioxide (5–6 mol of CO_2 per 100 mol of $Ru(bpy)_3^{3+}$ taken) is produced over the entire pH range, 0 to 12. In addition, modified $Ru(bpy)_3^{2+}$-like complexes whose yields (0.2–5.9 mol of Ru per 100 mol of $Ru(bpy)_3^{3+}$ taken) are a function of pH have been identified as products by high-performance liquid chromatographic analysis of the product solutions. The latter have been partially characterized by electrochemical and spectroscopic techniques and are not formed when sufficient Co^{2+}_{aq} (which catalyzes O_2 formation) is added to the reaction mixture. At pH 7, near stoichiometric O_2 formation is found for $(0.01\text{–}1.0) \times 10^{-3}$ M initial $Ru(bpy)_3^{3+}$ when the Co(II) catalyst concentration is $\simeq 0.1$ $[Ru(III)]_0$ and added [Ru(II)] is ≤ 10 $[Ru(III)]_0$. Kinetic studies as a function of pH, [Co(II)], $Ru(bpy)_3^{3+}$, and $Ru(bpy)_3^{2+}$ give the rate law $-d[Ru(III)]/dt = k[Ru(III)]^2[Co(II)]/[Ru(II)][H^+]^2$ ($k = 5.3 \times 10^{-10}$ M s^{-1} at 25 °C, 0.1 M ionic strength, pH 6.5–7.2) thus implicating a Co(IV) species as a crucial intermediate in O_2 formation. Irradiation of $Ru(bpy)_3^{3+}$ solutions with red light ($\lambda = 660 \pm 30$ nm) accelerates the reduction of $Ru(bpy)_3^{3+}$; the quantum yields for Ru(II) and CO_2 formation are 7×10^{-5} and 2.8×10^{-6} mol/einstein, respectively, in 4 M H_2SO_4 or CF_3SO_3H and 2×10^{-4} and 1.1×10^{-5} mol/einstein, respectively, in 1 M H_2SO_4 or CF_3SO_3H.

The reduction of $Ru(bpy)_3^{3+}$ in aqueous solution is a reaction of considerable current interest[1,2] since eq 1, in which water is oxidized to O_2, forms part of a scheme for water photodecomposition when combined with eq 2. Despite the desirability of

$$Ru(bpy)_3^{3+} + {}^1/_2H_2O \rightarrow Ru(bpy)_3^{2+} + {}^1/_4O_2 + {}^1/_2H^+ \quad (1)$$

$$Ru(bpy)_3^{2+} + H^+ \rightarrow Ru(bpy)_3^{3+} + {}^1/_2H_2 \quad (2)$$

eq 1, O_2 is formed stoichiometrically only in the presence of added catalysts such as Co^{2+}_{aq},[3,4] ruthenium complexes,[5,6] and metal oxide suspensions, and even then O_2 formation is more the exception than the rule.[7,8] Reduction of $Ru(bpy)_3^{3+}$ to $Ru(bpy)_3^{2+}$ occurs in aqueous media without O_2 formation over a wide range of conditions, and the nature of the oxidized products and the mechanism of their formation is of some interest. Similar behavior has been found for the analogous Fe(III) and Os(III) complexes.[9-11] Earlier preliminary studies of the products in the $Ru(bpy)_3^{3+}$ system showed that most (>90%) of the ruthenium-containing product is $Ru(bpy)_3^{2+}$ even when no O_2 is produced.[1] Here we have used high-performance liquid chromatographic techniques[12] to separate the other complexes produced in the reaction and have also identified CO_2 as a product of the decomposition.[13] In addition we have investigated the photoreduction of $Ru(bpy)_3^{3+}$ in acid media and find similar products for both thermal and photochemical paths. Finally, we have studied the Co(II) catalysis of O_2 formation by $Ru(bpy)_3^{3+}$ and, from the rate law in the neighborhood of pH 7, find that Co(IV) is implicated as an intermediate in the catalytic sequence.[4]

Experimental Section

Materials. $[Ru(bpy)_3]Cl_2 \cdot 6H_2O$ (G. F. Smith) was recrystallized twice from water. $[Ru(bpy)_3](ClO_4)_2$ was prepared by adding 4 M $HClO_4$ to an aqueous solution of $[Ru(bpy)_3]Cl_2$. The perchlorate salt was separated by filtration and dissolved in 0.5 M H_2SO_4. A scoop of PbO_2 was added, and the solution was stirred at room temperature and filtered through a fine frit. The perchlorate concentration of the filtrate was adjusted to ~2 M by the dropwise addition of $HClO_4$, and the solution was then cooled in an ice bath. Green crystals of $[Ru(bpy)_3](ClO_4)_3$ rapidly formed and were recrystallized from 4 M $HClO_4$ at 0 °C.

The complex $[Ru(bpy)_2(bpyO)](PF_6)_2$ (bpyO is bipyridine *N*-oxide, prepared via reaction of bpy with H_2O_2 in glacial acetic acid[14a]) was synthesized from $Ru(bpy)_2(dme)_2^{2+}$ (dme = dimethoxyethane)[14b] and bpyO under dry, anaerobic conditions. The chloride salt $[Ru(bpy)_2(bpyO)]Cl_2$ was isolated by treating a solution of the PF_6^- salt in acetone with tetrabutylammonium chloride. The material is extremely photosensitive and its photochemistry is currently under detailed study. IR (cm^{-1}) (chloride salt, KBr pellet): ν_{NO} 1226 (vs), 1240 (s), 1228 (sh); δ_{NO} 839 (vs).[14c]

Puratronic grade $CoSO_4$ was obtained from Johnson Matthey. Peroxide solutions were prepared by dilution of a commercial 30% solution and standardized from the absorbance decreases resulting when known

(1) Creutz, C.; Sutin, N. *Proc. Natl. Acad. Sci. U.S.A.* **1975**, *72*, 2858.
(2) Lehn, J. M.; Sauvage, J. P.; Ziessel, R. *Nouv. J. Chim.* **1979**, *3*, 423.
(3) Shafirovich, V. Ya.; Khannanov, N. K.; Strelets, V. V. *Nouv. J. Chim.* **1980**, *4*, 81.
(4) Brunschwig, B. S.; Chou, M. H.; Creutz, C.; Ghosh, P.; Sutin, N. *J. Am. Chem. Soc.* **1983**, *105*, 4832.
(5) Gersten, S. W.; Samuels, G. J.; Meyer, T. J. *J. Am. Chem. Soc.* **1982**, *104*, 4029.
(6) Goswami, S.; Chrakravarty, A. R.; Chakravorty, A. *J. Chem. Soc., Chem. Commun.* **1982**, 1288.
(7) Lehn, J. M.; Sauvage, J. P.; Ziessel, R. *Nouv. J. Chim.* **1980**, *4*, 355.
(8) Kiwi, J.; Kalyanasundaram, K.; Grätzel, M. *Struct. Bonding (Berlin)* **1982**, *49*, 37.
(9) Nord, G.; Wernberg, O. *J. Chem. Soc., Dalton Trans.* **1972**, 866.
(10) Nord, G.; Wernberg, O. *J. Chem. Soc., Dalton Trans.* **1975**, 845.
(11) Nord, G.; Pedersen, B.; Bjergbakke, E. *J. Am. Chem. Soc.* **1983**, *105*, 1913.
(12) Valenty, S. J.; Behnken, P. E. *Anal. Chem.* **1978**, *50*, 834.
(13) The formation of CO_2 is also reported by: Shafirovich, V. Ya.; Strelets, V. V. *Nouv. J. Chim.* **1982**, *6*, 183. CO_2 is produced in even higher yield in the $Ni(bpy)_3^{3+}$ system (S.-F. Chan, work in progress).
(14) (a) Murase, I. *Nippon Kagaku Zasshi* **1966**, *77*, 682; *Chem. Abstr.* **1958**, *52*, 9100a. (b) Connor, J. A.; Meyer, T. J.; Sullivan, B. P. *Inorg. Chem.* **1979**, *18*, 1388. (c) See: Speca, A. N.; Karayannis, N. M.; Pytlewski, L. L.; Winters, L. J.; Kandasamy, D. *Inorg. Chem.* **1973**, *12*, 1221.

0002-7863/84/1506-4772$01.50/0

amounts were mixed with excess Ce(IV) (ϵ = 5880 M^{-1} cm^{-1} at 320 nm).

Product Analysis. (A) Dioxygen. Early work was carried out with a Yellow Springs Model 53 oxygen monitor. In such experiments 2 mL of 2×10^{-3} M $Ru(bpy)_3^{3+}$ in 10^{-3} M H_2SO_4 was bubbled with argon in the monitor's cell and then 2 mL of deaerated buffer was syringed into the cell, with stirring. The meter response was calibrated against air-saturated water. Alternatively, gas chromatography was used to analyze O_2 in the gas phase: 7 mL of 2×10^{-3} M $Ru(bpy)_3^{3+}$ dissolved in 10^{-3} M H_2SO_4 was placed in a serum bottle and bubbled with argon; 7 mL of deaerated buffer was then added to the Ru(III) solution with stirring. The gas phase (1 mL) above the solution was analyzed by gas chromatography (2 m × 0.3 cm Molecular Sieve 5A column mounted in a Varian Series 1400 gas chromatograph equipped with a thermal conductivity detector; Ar carrier gas). Since correction for leaked air (detected by the presence of an N_2 peak) proved a complication to these measurements, an "on-line" technique was finally used as the method of choice: 7 mL of buffer and 7 mL of 2×10^{-3} M $Ru(bpy)_3^{3+}$ in 10^{-3} M H_2SO_4 were bubbled with argon in different arms of an H cell fitted with serum-cap-topped stopcocks. Polythene tubing threaded through the serum caps provided the argon inlets. One stopcock (a three way) was fitted with a 10/30 female joint which could be attached to the gas chromatograph via an adapted Valvco 6-port rotary valve containing a 0.5-mL-sample loop. After removal of air, the argon inlets and outlets were removed, the stopcocks were closed, and the vessel was tilted and then shaken back and forth to mix the buffer with the Ru(III). The mixture was stirred. To sample O_2, the flask was opened to the evacuated sample loop of the rotary valve and then injected onto the column with use of the Ar carrier gas. The method was calibrated with Ce^{IV}–H_2O_2 and/or by injecting known O_2 volumes (typically 5 μL) into argon-swept reactant solutions, sampling, and determining the peak heights obtained. The O_2 yields determined for $[Ru(III)]_0 < 2 \times 10^{-4}$ M were measured "on-line" with larger reactant volumes (50–100 mL) and with He carrier gas.

(B) Carbon Dioxide. Carbon dioxide was analyzed by gas chromatography (Varian Series 1400 gas chromatograph, 4 m × 0.3 cm Chromosorb 102 column, argon carrier gas). For the thermal or photochemical experiments in acid solution 1 mL of the ca. 20-mL gas phase above 20 mL of solution was sampled by syringe directly after reaction. Solutions run at higher pH were acidified before CO_2 analysis. A typical experiment for the detection of CO_2 formed in the $Ru(bpy)_3^{3+}$ reduction at pH 9 was as follows: 5 mL of a freshly prepared 0.05 M borate buffer was placed in one arm of a two-arm cell and 35 mg of $[Ru(bpy)_3](ClO_4)_3$ was placed in the other arm. After purging the cell with argon, 5 mL of deaerated 10^{-3} M H_2SO_4 was added to dissolve the $[Ru(bpy)_3](ClO_4)_3$. The $Ru(bpy)_3^{3+}$ solution was then added to the buffer solution in the cell. After the reaction had proceeded to completion, 5 mL of deaerated 4 M H_2SO_4 was added to the free side arm and the contents of the cell were mixed by vigorous shaking. An identical blank experiment was performed in an identical H cell, with the $Ru(bpy)_3^{3+}$ being omitted. The gaseous CO_2 was then analyzed as above. The CO_2 detected was calibrated against standard $NaHCO_3$ plus acid or by injecting known volumes of CO_2 into Ar-purged, reacted solution.

(C) Solution Products. Reduced $Ru(bpy)_3^{3+}$ solutions were prepared as described above and as follows. **(a) Reduction with Fe^{2+} in acid solutions**: $Ru(bpy)_3^{3+}$ in 10^{-3} M H_2SO_4 was reduced with a 2-fold excess of Fe(II) in 10^{-3} M H_2SO_4. This solution was then added to an appropriately buffered solution to serve as a control. **(b) Reduction with water over a wide pH range**: 1 mL of 10^{-2} or 10^{-3} M $Ru(bpy)_3^{3+}$ in 10^{-3} M H_2SO_4 was added to 9 mL of buffer solution. Phosphate buffer was used for the pH range 6.5–8.0, borate buffer was used at pH 9.0, and purified NaOH was used for the pH 12–14 solutions. **(c) Reduction in the presence of Co(II) in the pH range 6.5–9.0**: the procedure used here was identical with that described in (b) except that varying amounts of cobalt(II) sulfate were added to the solutions of $Ru(bpy)_3^{3+}$ in 10^{-3} M H_2SO_4.

Separation of the solution products was achieved by means of reverse-phase ion-pair chromatography.[12] Product solutions (typically 0.1 mL of 1 mM solution) were injected onto a Whatman C-18 column (Partisil ODS-3) mounted in a Perkin-Elmer Series 2 dual pump L.C. system. The compounds were detected with a variable wavelength Perkin-Elmer L.C. 85 UV–vis detector and the chromatogram recorded. The mobile phase was comprised of a strong solvent A (40% THF, pH 3.0) and a weak solvent B (5% THF, pH 3.0). Both A and B contained 0.005 M ion-pairing agent; optimum resolution was obtained with octanesulfonic acid (sodium salt) as the ion-pairing agent. The solutions were buffered with acetate (0.1 M), filtered through 0.5-μm filter paper and a 0.5-μm Millipore FH (organic) filter, and then stirred for a few minutes while several cycles of vacuum followed by helium purge were carried out. The latter procedure helped to prevent bubble formation in the L.C. system. Good separation was achieved when elution was carried out starting with 20% A and applying a continuous gradient (2% A/min) at a flow rate of 1.5 mL/min.

The potential product $Ru(bpy)_2(bpyO)^{2+}$ was found to have an elution time identical with that of $Ru(bpy)_3^{2+}$ under the standard chromatographic conditions. It was, however, possible to quantitatively determine the bipyridine *N*-oxide complex present as $\geq$0.5% of the ruthenium in known $Ru(bpy)_3^{2+}/Ru(bpy)_2(bpyO)^{2+}$ mixtures by stopping the flow and determining the absorbances at several wavelengths (e.g., 420, 450, 510 nm) where the molar absorptivities of the two complexes differ substantially. Therefore, comparisons of absorbance ratios of known and actual product mixtures at several wavelengths were used to determine $Ru(bpy)_2(bpyO)^{2+}$ in the reaction product solutions.

Preparative scale chromatography was performed on a Whatman Magnum 20-ODS-3 column following concentration of the side products with Waters Associates C-18 Sep-Pak cartridges. The cartridges were equilibrated by a prewash with ~3 mL of the acetonitrile followed by a rinse with ~10 mL of water. Aqueous solutions of the metal complexes containing 15–30 mg of the ion-pairing agent were then passed through the cartridges. The desired components were then eluted with aqueous THF (the larger the percent of THF in the mixture, the more facile the elution). To prepare the solids, the desired fraction from preparative HPLC was concentrated on a rotary evaporator, loaded onto a Sep-Pak, eluted with THF (to remove acetate, excess octanesulfonate, and other salts), and evaporated to dryness. The chloride of side-product ***1*** was prepared by dissolving the octanesulfonate salt so generated in water, passing the solution through Dowex 1-X8 anion exchange resin in the chloride form, and evaporating the resulting solution to dryness.

In a number of experiments, O_2, CO_2, and HPLC analyses were carried out on the same product mixture: 7.5-mL buffer and solid $[Ru(bpy)_3](ClO_4)_3$ were placed in separate arms of an H cell and subjected to an Ar purge for ~45 min and 7.5 mL of deaerated 1×10^{-3} M H_2SO_4 (containing $CoSO_4$, in some instances) was transferred by syringe (Pt needle) into the $Ru(bpy)_3^{3+}$ arm. The solutions were mixed and analyzed on-line to the gas chromatograph as described above. Next an ~0.5-mL solution was removed for HPLC analysis (within 1 h of sampling) as described above. Finally 5 mL of 4 M deaerated H_2SO_4 was added to the empty arm and mixed with the product solution. The gas above the resulting solution was analyzed for CO_2 as described earlier.

(D) *Ru(bpy)$_3^{2+}$. The chemiluminescence yield (the excited-state $*Ru(bpy)_3^{2+}$ is a product) was measured at high pH on a Durrum stopped-flow spectrophotometer. The photomultiplier tube (Hamamatsu R376) was mounted in the fluorescence configuration, and a Corning filter CS2-73 (570-nm cutoff) was placed between the observation tube and the photomultiplier. A typical yield measurement was made at 5.1 × 10^{-5} M $Ru(bpy)_3^{3+}$ and 0.2 M NaOH (μ = 1 M, 25 °C) with deaerated solutions. Under these conditions, the emitted light intensity (monitored on the oscilloscope as the voltage P_t) has an exponential time dependence, $P_t = P_0 \exp(-k_{obsd}t)$, where P_0 is the initial voltage and k_{obsd} is the pseudo-first-order rate constant for the disappearance of the emission. The integral under the oscilloscope trace is therefore P_0/k_{obsd} and is proportional to the total number of photons $(N_{h\nu})_{tot}$ (in einsteins) generated in the reaction (eq 3) where a_1 is a proportionality constant

$$(N_{h\nu})_{tot} = a_1 P_0 / k_{obsd} \quad (3)$$

(einstein V^{-1} s^{-1}). If it is assumed that the yield of photons from the excited state generated in the $Ru(bpy)_3^{3+}$ reduction is the same as the emission quantum yield of photoexcited $Ru(bpy)_3^{2+}$ (ϕ_{em} = 0.042),[15] then the total number of moles of excited-state N* generated in the reaction volume V (in liters) is given by eq 4 and the concentration of excited $Ru(bpy)_3^{2+}$ produced in the reaction $[*Ru(bpy)_3^{2+}]_{tot}$ is given by eq 5.

$$N^* = a_1 P_0 / k_{obsd} \phi_{em} \quad (4)$$

$$[*Ru(bpy)_3^{2+}]_{tot} = a_1 P_0 / k_{obsd} \phi_{em} V \quad (5)$$

Consequently, the excited-state yield $\phi^* = [*Ru(bpy)_3^{2+}]_{tot}/[Ru(bpy)_3^{3+}]_0$ can be evaluated if the value of a_1 is known. The procedure described in the supplementary material yielded $a_1/V\phi_{em} = 8.14 \times 10^{-8}$ einstein V^{-1} L^{-1} s^{-1}. Substituting this result into eq 5 gives $[*Ru(bpy)_3^{2+}]_{tot} = (8.14 \times 10^{-8}) P_0/k_{obsd}$. The P_0 and k_{obsd} values were typically 15 V and 55 s^{-1}, respectively, for 5.1×10^{-5} M $Ru(bpy)_3^{3+}$ and 0.2 M NaOH.

Kinetics. Experiments at high pH or at pH 7 with high Co(II) were carried out on a thermostated Durrum stopped-flow spectrophotometer. The slower runs were monitored on thermostated Cary 17 or 210 spectrophotometers at 675 or 452 nm. For experiments at pH >6, $Ru(bpy)_3^{3+}$ dissolved in 1×10^{-3} M H_2SO_4 was usually mixed with an equal

(15) Van Houten, J.; Watts, R. J. *J. Am. Chem. Soc.* **1975**, *97*, 3843.

Table I. Product Yields (mol per 100 mol of $Ru(bpy)_3^{3+}$ taken) with 1.0×10^{-3} M $Ru(bpy)_3^{3+}$ as a Function of pH[a]

product[b]	0[c]	2.5	4.7[c]	6.5	7.0	7.5	8.0	9.0	12	13[c,d]
O_2	<0.1	<0.2	0.4		0.6			1.0		0.6 (–)
CO_2	5		7.5		4.6			6.5	5	0[e] (–)
0	0.0	0.0	0.0						0.0	0.0 (0.0)
1	0.0	0.0	0.0	0.8	3.4	5.6	5.9	0.0	0.0	0.0 (0.0)
2	0.0	0.3	0.3	1.0	1.2	1.5	1.8	1.2	3.5	2.6 (0.9)
3	0.6	0.9	0.3	0.6	1.0	1.2	1.6	5.9	2.0	0.5 (0.5)
4	0.5	1.5	0.6	3.0	2.8	2.0	1.8	0.5	0.3	0.2 (0.3)
5	0.0	0.0	0.0	0.1	0.2	0.3	0.3	0.0	0.7	0.5 (0.2)
6	0.0	3.2	0.0	0.7	0.6	0.6	0.5	0.7	0.3	0.0 (3.0)
7	1.3	0.0	0.8	1.1	2.8	2.9	1.7	0.0	2.6	2.6 (4.0)
7A[f]	0.0	0.0	0.0	0.0	0.0	0.0	0.0	0.0	0.0	3.5 (4.6)
8	0.0	0.0	0.0	0.4	0.5	0.5	0.2	0.0	0.0	0.1 (0.0)
9	0.0	0.0	0.0	0.0	0.4	0.4	0.1	0.0	0.0	0.0 (0.0)
$*Ru(bpy)_3^{2+}$									0.01	0.04

[a] Unless otherwise noted the yields of the ruthenium-containing side-products ***1–9*** were determined for solutions in which air was not excluded and O_2 and CO_2 were measured in additional experiments. The yields of ***1–9*** are based on 450-nm peak heights, corrected for the ϵ of the product at 450 nm (Table II), and are normalized by the $Ru(bpy)_3^{2+}$ chromatogram peak height. [b] The following were used: pH 0, 1 M H_2SO_4; pH 2.5, 1×10^{-3} M H_2SO_4; pH 4.7, 0.1 M acetate buffer; pH 6–8, 0.025 M phosphate buffer; pH 9, 0.025 M borate buffer; pH 12, 0.01 M NaOH; pH 13, 0.1 M NaOH. [c] All the analyses were performed on the same air-free sample. [d] Numbers given in parentheses were obtained for a product sample prepared by mixing equal volumes of 0.2 M NaOH and 2.0×10^{-4} M $Ru(bpy)_3^{3+}$ in a stopped-flow machine. [e] Some CO_2 may be produced, but the "yield" (7.5) was the same as for the blank (0.1 M NaOH, no Ru(III)) which is quite large at high pH. [f] The yield given assumes ϵ_{450} for ***7A*** is identical with that of $Ru(bpy)_3^{2+}$.

volume of buffer brought to temperature in the 1- or 2-cm cell. For <1 $\times 10^{-4}$ M $Ru(bpy)_3^{3+}$ and 675-nm monitoring, 0.5–1 mL of the stock $Ru(bpy)_3^{3+}$ was added to ~30 mL of deaerated buffer contained in a stirred 10-cm cell. The absorbance–time data were digitized and read on-line (stopped flow) or by an x–y digitizing tablet (Cary traces) into a PDP 11/23 and analyzed by nonlinear least-squares fitting routines.

Photochemical Reduction of $Ru(bpy)_3^{3+}$. Two identical 2 × 2 cm square glass cells containing 20 mL of $(1–2) \times 10^{-3}$ M $Ru(bpy)_3^{3+}$ in 1–4 M H_2SO_4 or CF_3SO_3H were deaerated by argon bubbling and then one cell was irradiated with red light ($\lambda = 660 \pm 30$ nm, Oriel LP630 long-pass colored-glass and 35-5495-4 MZF 7-1 short-pass interference filters) from a 450-W xenon lamp and the other was wrapped in aluminum foil and served as a control. Both cells were immersed in the same water bath to eliminate temperature effects, and each was fitted with a stopcock and serum cap to permit sampling of the gas phase. The light intensity was determined by use of an Eppley Coblentz-type circular thermopile (8-junction, air case, sensitivity ~6.3 mW/mV). The thermopile's calibration was checked at 450 nm by ferrioxalate actinometry (agreement was within ~15%). The response of the thermopile was found to be linear below ~1 mV. The light intensity varied less than 10% from day to day and was $\sim 6 \times 10^{-7}$ einstein s^{-1} at 660 nm.

Instrumentation for Spectroscopy and Electrochemistry. Absorption spectra were recorded on Cary 17 or 210 spectrophotometers. IR spectra were run on a Nicolet MX-1 FT spectrometer and NMR spectra were recorded on a Varian CFT-20 machine. Instrumentation for cyclic voltammetry consisted of a PAR Model 173 potentiostat, a Model 175 universal programmer, and a Model 179 coulometer. The voltammograms were recorded on a Hewlett-Packard x–y recorder. Glassy carbon was employed as the working electrode in a conventional three-electrode arrangement with a saturated calomel reference electrode.

Results

Spontaneous Reduction of $Ru(bpy)_3^{3+}$ in Water. Products. High-performance liquid chromatography (HPLC) enabled the separation of $Ru(bpy)_3^{2+}$ from some ten ruthenium(II)-containing side products. Figure 1, a chromatogram obtained by monitoring at 450 nm illustrates the complicated distribution obtained and defines the side-product numbering scheme used. Only the main peak $Ru(bpy)_3^{2+}$ was observed with Fe^{2+}_{aq} as reducing agent. By use of preparative chromatography the main product was isolated as a perchlorate salt and its cyclic voltammogram and UV–vis, IR, and NMR spectra were recorded. Its molar absorptivity was obtained by measuring the absorbance of a solution for which the ruthenium concentration had been determined by atomic absorption. (The latter method may give Ru analyses up to 15% low, depending upon the complex.) On the basis of comparisons with an authentic sample of $Ru(bpy)_3^{2+}$, it is concluded that the main product of the reduction is indeed $Ru(bpy)_3^{2+}$. No H/D exchange was detected in the product when perdeuterio-$Ru(bpy)_3^{3+}$ (1×10^{-3} M) reacted with 0.1 M NaOH (upper limit from NMR and IR intensities: ≤5% C–D exchange). In addition, gas chromatography of acidified solutions revealed that CO_2 is

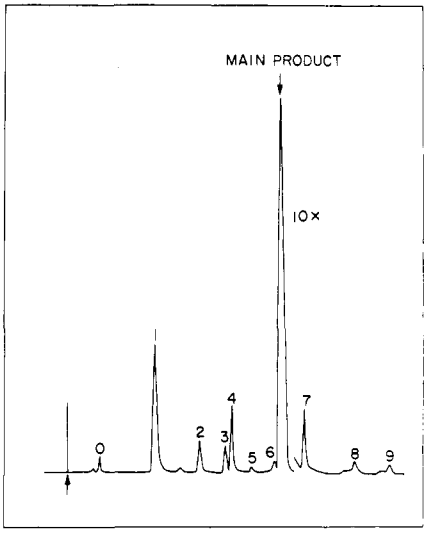

Figure 1. Liquid chromatographic separation of the products of the reduction of $Ru(bpy)_3^{3+}$ in 0.025 M phosphate buffer, pH 7.

a product[13] and confirmed that essentially no O_2 or H_2O_2 (estimated as O_2 following addition of Ce(IV) to acidified solutions) is produced.

The product distributions obtained with initially 1×10^{-3} M $Ru(bpy)_3^{3+}$ at pH 0 to 13 are presented in Table I. The yield of $*Ru(bpy)_3^{2+}$ (determined at much lower $Ru(bpy)_3^{3+}$) is also included.

The spectral and electrochemical properties of the major side products are given in Table II. All absorb strongly in the visible region, exhibiting spectra similar to that of $Ru(bpy)_3^{2+}$. HPLC chromatograms obtained with 280-nm monitoring differed little from those obtained at 450 nm indicating that the UV spectra of the side products also do not differ substantially from that of $Ru(bpy)_3^{2+}$. In addition, no new peaks were discernible under UV detection, ruling out the presence of free bipyridine (or products resembling it). For reduction at pH 6–12, 6–8% of the initial $Ru(bpy)_3^{3+}$ is converted to side products. Most of the side products are unstable in aqueous solution, and react over several days to give either changes in the relative amounts of the side products or, in other cases, e.g., with product ***1***, formation of a new species ***1′*** which has a similar retention time to side-product ***8***. Due to this instability, the data were obtained before any significant decomposition of the side products had occurred. In addition, side-products ***1*** and ***2*** were isolated as solids and found to be stable in the solid state.

Table II. Spectral and Electrochemical Properties of the Products Formed in the Thermal Reduction of $Ru(bpy)_3^{3+}$

product	λ_{max},[a] nm	ϵ_{max}[b]	$E°$ in CH_3CN, V vs. SCE	$E°$ in H_2O, V vs. NHE
1	455	1.30×10^4	1.22	1.20
1'[c]	456	1.41×10^4		
2	468	1.01×10^4	0.85	0.89
3	468	1.06×10^4	0.84	0.89
4	460	1.06×10^4	0.81	
5	462	0.75×10^4	0.54, 0.82	
6	466		0.50	
$Ru(bpy)_3^{2+}$	452	1.42×10^4	1.29	1.26
7	457	1.03×10^4	0.81	0.86
8	470, 380			
$Ru(bpy)_2L^{2+}$[d]	465	0.77×10^4	0.96	

[a] In H_2O, pH 7. The spectra were not sensitive to pH (pH 2 and 12). [b] The ruthenium concentrations upon which the molar absorptivities of the side products are based were determined by atomic absorption and could be low by 15% depending upon the complex. [c] Side-product ***1'*** is formed from ***1*** on standing and has approximately the same retention time as ***8***. [d] L = bipyridine *N*-oxide. This complex is *not* observed as a side product (≤0.5% of Ru); its properties are included only for comparison purposes. The retention time of this complex is the same as that of $Ru(bpy)_3^{2+}$.

Because bipyridine *N*-oxide was detected in the $Fe(bpy)_3^{3+}/OH^-$ reaction products,[11] both free and bound bpyO were sought in the Ru(III)–product mixtures. As noted above, only CO_2 and Ru(II)-containing products were found (no free bpyO). Thus the complex $Ru(bpy)_2(bpyO)^{2+}$ was prepared and characterized; its properties are compared with those of the reaction side products in Table II. It is evident that none of the side-products ***1–9*** is $Ru(bpy)_2(bpyO)^{2+}$. In fact the latter has a retention time identical with that of $Ru(bpy)_3^{2+}$. For this reason the "$Ru(bpy)_3^{2+}$" fraction in the reaction mixtures was examined at several wavelengths and the absorbance ratios were compared with those for known $Ru(bpy)_3^{2+}/Ru(bpy)_2(bpyO)^{2+}$ mixtures. From these comparisons $Ru(bpy)_2(bpyO)^{2+}$ is ≤0.5% of the $Ru(bpy)_3^{2+}$ fraction. In addition, the *N*-oxide complex was added to the reaction mixtures both before and after mixing Ru(III) and buffer (at 10% and 1% of $Ru(bpy)_3^{3+}$) and was detected (as above) unchanged in the product. Thus there is no evidence that either free or bound bpyO is produced in the $Ru(bpy)_3^{3+}/OH^-$ reaction.

The NMR spectra of $Ru(bpy)_3^{2+}$, ***1***, and ***2*** are presented in Figure 2. That of ***1*** has broad envelopes in the general region where the hydrogens of the bpy ligands in $Ru(bpy)_3^{2+}$ occur with well-defined coupling patterns. The loss of resolution results from overlap of the chemically shifted proton signals (arising from partial oxidation of one of the bipyridines) with the signals from the remaining bipyridines. Additional complications are introduced by the lowering of the molecular symmetry. The IR spectrum of the chloride salts of ***1*** and $Ru(bpy)_3^{2+}$ differ somewhat, and the spectrum of ***1*** is consistent with the presence of an aromatic C–OH group and unmodified bpy ligands: 3400 cm^{-1} (br), O–H stretch or H_2O; 3035, 3020, 3035 cm^{-1}, C–H stretch; 1600, 1475, 1464, 1443, 1422 cm^{-1}, C=C stretch; 1331 (weak), O–H bend; 1238 (s), 1122 (vs) cm^{-1}, C–O stretch; 1027 (s) cm^{-1}, C–H bend; 928 cm^{-1}, C–H bend. It is evident from Table II that the spectra and reduction potentials of ***1*** and ***1'*** are similar to those of $Ru(bpy)_3^{2+}$, suggesting that these products contain one modified bpy, perhaps a hydroxybipyridine group. The observation that ***1*** is present in proportionately higher amounts during the initial stages of the reaction (vide infra) further supports this interpretation, as does the short HPLC retention time of ***1***: if ***1*** contains a hydroxybipyridine group the considerably shorter retention time could result from the lowered charge resulting from proton loss.

The NMR spectrum of ***2*** (Figure 2) suggests considerable degradation of at least one bipyridine group, while the infrared spectrum of ***2*** suggests the presence of C=C–C=O: 1642 cm^{-1} (s), C=O; 1590, 1460–1410 cm^{-1}, C=C 1330–1260 cm^{-1}, C–C–C stretch/bend. The sharp band at 843 cm^{-1} is similar in position to the δ_{N-O} mode (839 cm^{-1} vs) of the coordinated bipyridine *N*-oxide ligand (ν_{N-O} at 1240–1220 cm^{-1}) but much lower in intensity. Its visible spectrum (λ_{max} 468 nm) and $E_{1/2}$ (0.89 V) indicate that the metal center differs significantly from that of $Ru(bpy)_3^{2+}$ and may, in fact (like that in ***3***), resemble that of $Ru(bpy)_2(py)X^+$ (X = $CH_3CO_2^-$, NCS^-, etc.[16]), so that it is possible that the degradation is confined to one pyridine of a bipyridine molecule.

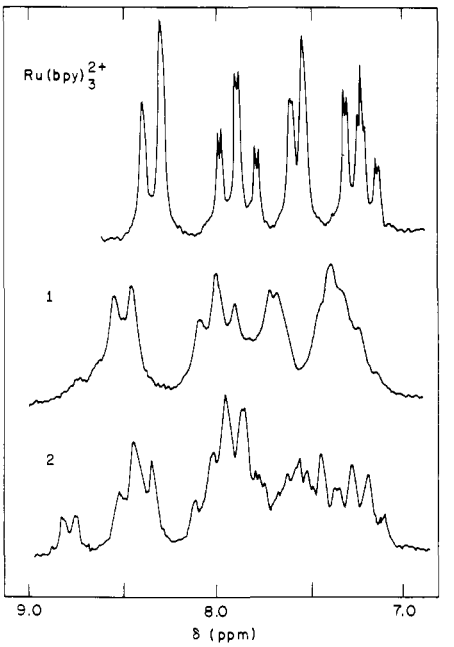

Figure 2. Proton NMR spectra of $Ru(bpy)_3^{2+}$, product ***1*** and product ***2*** in CD_3CN solvent.

The electrochemical properties of ***5*** are noteworthy. Two oxidation waves are found for ***5*** suggesting that both Ru(II)/Ru(III) and Ru(III)/Ru(IV) couples are accessible. Such behavior has been documented for the closely related $Ru(terpy)(bpy)H_2O$ and $Ru(bpy)_2(py)H_2O$ systems.[16]

It is apparent from Table I that, in contrast to $Ru(bpy)_3^{2+}$ and CO_2, the relative yields of the side products depend upon pH. The yield of product ***1*** is at a maximum near pH 7–8, the yield of ***2*** maximizes near pH 12, that of ***3*** is greatest pH 9, and ***4*** peaks somewhat below pH 7. The pH dependence of the yields of the other species is somewhat more complicated. As discussed previously[1] and in more detail in the next section, reduction of $Ru(bpy)_3^{3+}$ is initiated by hydroxide ion or water addition to the bound bipyridine and is followed by further reaction with OH^- and Ru(III) to give CO_2 and the degraded ruthenium(II) complexes detected by HPLC. The varying distributions of the side products result from non-rate-determining reactions whose relative rates depend upon OH^- and Ru(III). Several approaches were utilized in an effort to distinguish early degradation products from the later ones. In the first approach the reaction at pH 7 was intercepted after ~30% completion by the addition of Co(II) (reduction with Co(II) affords a clean chromatogram). The relative yields altered dramatically and considerably higher amounts of ***1*** were detected suggesting that this product is formed during the early stages of the reduction and that it undergoes subsequent reaction. In another approach experiments at high pH were carried out as a function of $Ru(bpy)_3^{3+}$ concentration. Remarkably, in these high-pH experiments no ***1*** was produced; instead the highest yield products with 1 mM $Ru(bpy)_3^{3+}$ were ***2*** and ***7***. As the Ru(III) concentration was dropped to 0.1×10^{-3}, 0.04×10^{-3}, and 0.02×10^{-3} M a distribution change was noted, but it involved increased yields of ***6*** and ***7*** and a decreased yield of ***2***. These observations are consistent with formulation of ***2*** as a "later" oxidation product, as is also suggested by its spectral parameters described above. Although the resemblance of the

(16) Durham, B.; Wilson, S. R.; Hodgson, D. J.; Meyer, T. J. *J. Am. Chem. Soc.* **1980**, *102*, 600.

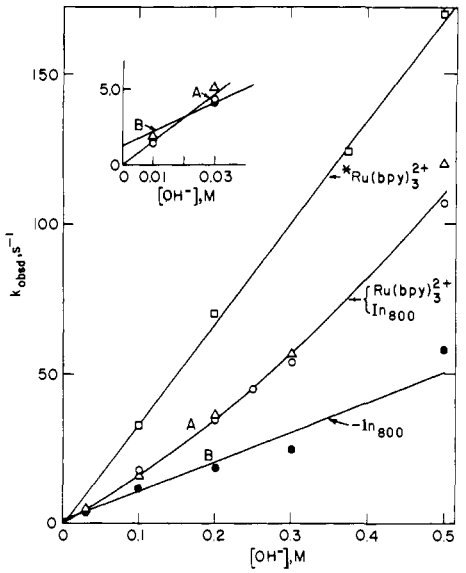

Figure 3. Kinetic data for the $Ru(bpy)_3^{3+}$–OH^- reaction obtained by the stopped-flow method; the pseudo-first-order rate constant k_{obsd} as a function of hydroxide ion concentration for (△) $Ru(bpy)_3^{2+}$ formation (452 nm), for (○) the formation and (●) the disappearance of an 800-nm-absorbing transient, and (□) the tail of chemiluminescence at 3×10^{-4} M $Ru(bpy)_3^{3+}$.

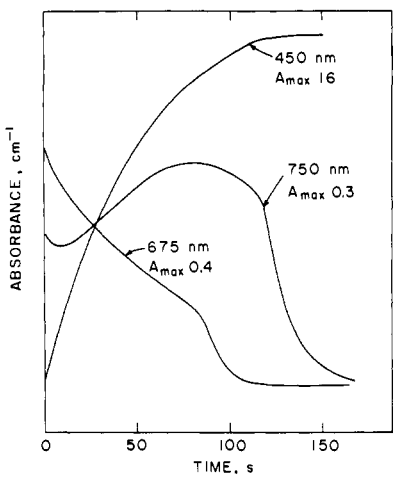

Figure 4. Absorbance–time profiles for initially 1.0×10^{-3} M $Ru(bpy)_3^{3+}$ in pH 7.0 (0.025 M phosphate) buffer. Note that the absorbance scales differ for the three wavelengths shown.

chromatographic properties of ***6*** and ***7*** to those of $Ru(bpy)_3^{2+}$ could be taken as evidence that the structures of ***6*** and ***7*** strongly resemble that of $Ru(bpy)_3^{2+}$, the low redox potentials found for these complexes rule out this possibility. Instead "tetra-" and "penta"-pyridine formulations (i.e., $Ru(bpy)_2L_2^{2+}$ and $Ru(bpy)_2(py)L^{2+}$)[16] provide more reasonable models for the electrochemical properties of ***6*** and ***7***, respectively. Although the structures assigned to the various side products must be regarded as tentative, the difference between the pH 7 and 13 distributions suggests that degradation of ***1*** can occur even at low Ru(III) provided the hydroxide ion concentration is sufficiently high.

Kinetics. In the dark the reduction of $Ru(bpy)_3^{3+}$ in acid solutions is extremely slow. The initial rate constants for $Ru(bpy)_3^{2+}$ formation in 2 mM $Ru(bpy)_3^{3+}$ are as follows: 1 M H_2SO_4, $\leq 1.0 \times 10^{-5}$ s^{-1}; 1 M CF_3SO_3H, $\leq 0.9 \times 10^{-5}$ s^{-1}; 4 M CF_3SO_3H, $\leq 1 \times 10^{-6}$ s^{-1}; 4 M H_2SO_4, $\leq 0.3 \times 10^{-6}$ s^{-1} at 25 °C.

The reaction of $(0.3–1.7) \times 10^{-4}$ M $Ru(bpy)_3^{3+}$ with hydroxide ion at pH ≥ 12 was followed by the stopped-flow technique[1]. Representative data are presented in Figure 3. Included are data for the pseudo-first-order production of $Ru(bpy)_3^{2+}$ determined at 450 nm, for the appearance and disappearance of an 800-nm-absorbing intermediate, and data for the tail of the chemiluminescence at high $Ru(bpy)_3^{3+}$ concentration. From the 450-nm data, assuming that $d[Ru(II)]/dt = -d[Ru(III)]/dt$, the experimental rate law is[1]

$$\frac{-d[Ru(III)]}{[Ru(III)]dt} = k_a[OH^-] + k_b[OH^-]^2 \qquad (6)$$

where $k_a = 1.5 \times 10^2$ M^{-1} s^{-1} and $k_b = 1.4 \times 10^2$ M^{-2} s^{-1} ($[OH^-] = 0.01–0.5$ M, 25 °C, 1 M ionic strength).[1]

As noted earlier,[1] the behavior found for buffered pH 7–10 solutions depends upon the initial $Ru(bpy)_3^{3+}$ concentration and the solution pH. As shown in Figure 4, the behavior observed is also wavelength dependent with a 700–800-nm-absorbing intermediate complicating the profile as was also seen at high pH. In general the rates measured are more rapid than would be predicted from eq 6. Typical rate constants obtained at 675 nm for initially $(0.1–10) \times 10^{-4}$ M $Ru(bpy)_3^{3+}$ solutions at 1 M ionic strength and 25 °C are as follows: pH 10 (carbonate), $(3–7) \times 10^{-2}$ s^{-1}; pH 9 (borate), $(0.8–1.4) \times 10^{-2}$ s^{-1}; pH 7 (phosphate), $(0.3–3.5) \times 10^{-3}$ s^{-1}. The rate ranges reflect variation with [Ru(III)]; individual runs are reproducible when freshly prepared stock $Ru(bpy)_3^{3+}$ solutions are used. Extensive experiments at pH 7, 0.1 M ionic strength ("blanks" for the added Co^{2+} runs described later), indicate that the $Ru(bpy)_3^{3+}$ decay rates increase somewhat when $Ru(bpy)_3^{2+}$ is added and as [Ru(III)] is increased (see supplementary material, Table I).

Chemiluminescence. The red emission observed when $Ru(bpy)_3^{3+}$ is mixed with aqueous sodium hydroxide has the same spectrum as the emission spectrum of $Ru(bpy)_3^{2+}$;[17] thus we have treated the emitting product as $*Ru(bpy)_3^{2+}$.[18] The chemiluminescence exhibits a complex hydroxide and Ru(III) dependence. With 0.01 M NaOH (μ = 1 M, Na_2SO_4, 25 °C) the chemiluminescence intensity P_t is described by $(P_t)^{-1} = (P_0)^{-1} + k_p t$ and occurs over ~50 ms or less even though the half-life for $Ru(bpy)_3^{3+}$ decay is ~500 ms. Under such conditions ($[Ru(bpy)_3^{3+}] = (0.1–2) \times 10^{-4}$ M) the yield of $*Ru(bpy)_3^{2+}$ is $\sim 1 \times 10^{-4}$ mol per mol of $Ru(bpy)_3^{3+}$ taken. With 0.1–0.3 M OH^- and $(1–3) \times 10^{-4}$ M $Ru(bpy)_3^{3+}$, μ = 1 M (Na_2SO_4), 25 °C, the chemiluminescence intensity exhibits a maximum at t = 0.002–0.1 s and then decays exponentially with $k_{obsd} = 3.4 \times 10^2$ $[OH^-]$ (data presented in Figure 3). The yield of $*Ru(bpy)_3^{2+}$ determined in 0.2 M NaOH is 3×10^{-4} mol per mol of $Ru(bpy)_3^{3+}$ taken. The chemiluminescence intensity was extremely sensitive to oxygen, being 30 times greater in argon-saturated than in oxygen-saturated solutions. (Simple quenching of $*Ru(bpy)_3^{2+}$ emission by O_2 would give only a factor of ~3.5 in the relative yields.) It was also noted that aged $Ru(bpy)_3^{3+}$ solutions produced very bright chemiluminescence when mixed with pH 7–10 buffers.

Photoreduction of $Ru(bpy)_3^{3+}$ in Acid Solutions. Since the lifetime of $Ru(bpy)_3^{3+}$ is 25 h or longer in strongly acidic media, photochemical experiments are feasible under such conditions. Photolysis was carried out with red light ($\lambda = 660 \pm 30$ nm) in the ligand-to-metal charge-transfer band of $Ru(bpy)_3^{3+}$ (λ_{max} 675 nm, ϵ 440 M^{-1} cm^{-1}). With $I_0 = 6 \times 10^{-7}$ einstein s^{-1}, the rate of $Ru(bpy)_3^{3+}$ disappearance is two to five times greater than in the dark, depending upon the medium used. At 25 °C the quantum yields for $Ru(bpy)_3^{3+}$ consumption (after correction for the dark reaction rates) are 2×10^{-4} in 1 M H_2SO_4 or CF_3SO_3H and 7×10^{-5} in 4 M H_2SO_4 or CF_3SO_3H. The products of the photoreduction were qualitatively the same as those formed in the dark: $Ru(bpy)_3^{2+}$, the main product, was identified by spectral (IR, NMR, UV–vis) and electrochemical analysis and through NMR studies of the products resulting from photoreduction of $Ru(bpy\text{-}d_8)_3^{3+}$ (no H was incorporated). As in the dark reduction,

(17) Lytle, F. E.; Hercules, D. M. *Photochem. Photobiol.* **1971**, *13*, 122.

(18) We have assumed that the luminescent product is indeed the metal-to-ligand charge-transfer excited state of $Ru(bpy)_3^{2+}$. However, since the emission spectra of $Ru(bpy)_3^{2+}$ and related complexes differ very little, it is conceivable that the luminescence arises instead from a side product, for example, $Ru(bpy)_2(bpy\text{-}OH)^{2+}$. (Note that our yield estimates are based upon the assumption that $Ru(bpy)_3^{2+}$ is the source of the emission since we have used the emission yield reported for $*Ru(bpy)_3^{2+}$ in calculating the excited-state yield.)

Table III. Product Yields (mol per 100 mol of $Ru(bpy)_3^{3+}$ taken) with 1.0×10^{-3} M $Ru(bpy)_3^{3+}$ in the Presence and Absence of Added $CoSO_4$[a]

	[Co(II)], M						
	pH 7.0[b]		pH 9.0[c]				
product[e]	0.0	1×10^{-4}	0.0[d]	10^{-7}	10^{-6}	10^{-5}	10^{-4}
O_2	0.6	13.8	1.0	4.7	13.7	32.5	14.9
CO_2	4.6	1.2	5.8				0.6
0	0.5	0.0	0.0	0.0	0.0	0.0	0.0
1	4.3	0.2	0.0	0.0	0.0	0.0	0.0
2	0.4	0.0	1.7	0.9	0.1	0.1	0.0
3	0.6	0.0	5.3	3.2	0.6	0.1	0.0
4	1.3	0.0	0.3	0.2	0.2	0.2	0.2
5	0.1	0.0	0.0	0.0	0.0	0.0	0.0
6	0.0	0.0	0.0	0.0	0.0	0.0	0.0
7	3.0	0.8	1.6	1.0	1.0	1.0	0.8
8	0.3	0.0	0.1	0.0	0.0	0.0	0.0
9	1.0	0.0	0.0	0.0	0.0	0.0	0.0

[a] Ambient temperature 22 ± 2 °C. The $[Ru(bpy)_3](ClO_4)_3$ solid used was <1 week old. All analyses were performed on the same sample prepared in an H cell (see Experimental Section). The O_2 yield was determined 1 h (or longer for slow reactions) after mixing of Ru(III) and buffer by direct injection onto the gas chromatograph. Then a 0.5-mL solution was withdrawn, of which 0.1 mL was injected onto the HPLC for side-product analysis. Finally 5 mL of 4 M H_2SO_4 (deaerated) was added to the solution in the cell and CO_2 was analyzed (1 mL of the ~25-mL gas phase) after 2 h of stirring. [b] The buffer was 0.25 M phosphate (sodium salts). [c] The buffer was 0.025 M borate from Allied lot GCDY 147. [d] Average of four separate determinations. [e] Products numbered ***0*** to ***9*** are the ruthenium-containing side products and are numbered in order of elution from the HPLC.

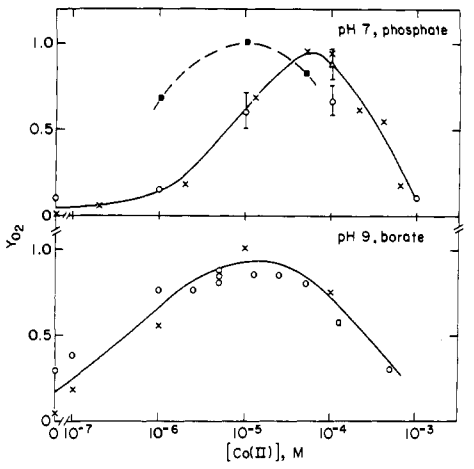

Figure 5. Dioxygen yields (eq 1) as a function of cobalt(II) concentration. Top: pH 7, 1×10^{-3} M $Ru(bpy)_3^{3+}$; (Δ) 0.03 M phosphate, (×) 0.125 M phosphate, (○) 0.025 M phosphate; (■) 2×10^{-4} M $Ru(bpy)_3^{3+}$, 0.025 M phosphate. Bottom: pH 9, 1×10^{-3} M $Ru(bpy)_3^{3+}$; (×) 0.025 M borate, (○) 0.1 M borate. Yields denoted with open circles were determined with the O_2 electrode; all others were determined by gas chromatography.

small quantities of other ruthenium-containing compounds and CO_2 were also produced. However, the CO_2 yields in the light-induced and dark reactions differed. The quantum yields for CO_2 formation are 1.1×10^{-5} in 1 M acid and 2.8×10^{-6} in the 4 M acid, corresponding to 0.06 and 0.04 mol of CO_2/mol of Ru(III) consumed in 1 and 4 M acid, respectively. In the dark the CO_2 yields were 0.02 and 0.2 mol of CO_2/mol of Ru(III) consumed in 1 and 4 M acid, respectively.

Reduction of $Ru(bpy)_3^{3+}$ in the Presence of Cobalt(II). Products. The results of our studies of the $Ru(bpy)_3^{3+}$ reaction products as a function of [Co(II)] and pH are presented in Table III, and O_2 yields at pH 7 and 9 are plotted as a function of [Co(II)] in Figure 5. The data in Table III show that, in the presence of Co(II), O_2 is formed at the expense of CO_2 and that only traces of ruthenium-containing side products persist when the O_2 yield is high. The HPLC chromatograms of pH 7, 1×10^{-3} M $Ru(bpy)_3^{3+}$–product solutions confirm that at 10^{-5} M Co(II) the non-degradative pathway is the dominant route. At 10^{-6} M Co(II), however, oxidative degradation of the ligand predominates. In addition, experiments with 1×10^{-4} M Ru(III) indicate that the competition between the two pathways is governed not so much by the absolute concentration of Co(II) as by the Ru(III)/Co(II) ratio: a solution containing 1×10^{-4} Ru(III) and 1×10^{-6} M Co(II) (pH 7) yields the same chromatogram as that obtained for a solution containing 1×10^{-3} M Ru(III) and 1×10^{-5} M Co(II) (pH 7). The dependence of O_2 yield on [Co(II)] at pH 7 shown in Figure 5 is in excellent agreement with the literature results,[3] being maximal between 10^{-5} and 10^{-4} M Co(II) when the initial $Ru(bpy)_3^{3+}$ concentration is millimolar. With 0.2×10^{-3} M $Ru(bpy)_3^{3+}$, O_2 is formed at high yield with even lower added Co(II) (points on broken line); even at 10^{-6} M Co(II) and O_2 yield is nearly 70% at pH 7. At pH 9, the maximum O_2 yield occurs at lower catalyst concentration, 10^{-6}–10^{-5} M Co(II), with 1×10^{-3} M $Ru(bpy)_3^{3+}$.

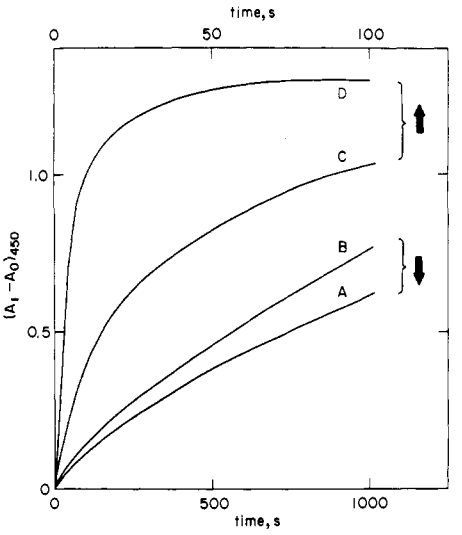

Figure 6. Absorbance–time profiles for $Ru(bpy)_3^{2+}$ formation at 450 nm at 25 °C in 0.025 M phosphate buffer. Initial conditions: (A) 1×10^{-4} M $Ru(bpy)_3^{3+}$; (B) 1×10^{-4} M $Ru(bpy)_3^{3+}$, 1×10^{-4} M $Ru(bpy)_3^{2+}$; (C) 1×10^{-4} M $Ru(bpy)_3^{3+}$, 1×10^{-4} M $Ru(bpy)_3^{2+}$, 3.5×10^{-6} M Co(II); (D) 1×10^{-4} M $Ru(bpy)_3^{3+}$, 3.5×10^{-6} M Co(II). Note that the time scale is a factor of ten faster for C and D (upper scale).

Kinetics. Kinetics studies were carried out in buffered pH 7–9 solutions at 25 °C with $(0.01–1.5) \times 10^{-3}$ M $Ru(bpy)_3^{3+}$ and $(1–100) \times 10^{-6}$ M $CoSO_4$ in 0.1 M ionic strength 0.025 M phosphate buffers.[4] The rate of $Ru(bpy)_3^{3+}$ disappearance was indeed enhanced by the addition of Co(II) as is illustrated in Figure 6. In contrast to the behavior in the absence of Co(II) (see Figure 4), the absorbance–time profile did not depend upon the wavelength used to monitor the reaction. The rates were pH sensitive and the time profiles were complicated, but analysis of the data in terms of a second-order $[Ru(bpy)_3^{3+}]$ dependence proved tractable once inhibition by the product $Ru(bpy)_3^{2+}$ was recognized as an important factor. As is shown at the upper right of Figure 7, the fit to first-order inhibition by $Ru(bpy)_3^{2+}$ is excellent over a wide range of conditions. However, as is shown in the lower left of Figure 7, the [Co(II)] dependence of the rates is complicated. For $[Ru(III)]_0 > 3 \times 10^{-4}$ M, increasing $[Ru(III)]_0$ at constant [Co(II)] leads to a smaller [Ru(II)] k_{obsd} value and increasing [Co(II)] at constant $[Ru(III)]_0$ gives rise to the curved plots shown in Figure 7. The behavior did not simplify in the high Ru(III) region: when the reaction of equimolar Ru(III) and Co(II) was studied by the stopped-flow technique, triphasic behavior was found, with most of the Ru(II) (450 nm) being produced in a rapid, apparently zero-order stage. Intense transient absorption at ~600 nm obscured the Ru(III) disappearance normally monitored at 675 nm and a black solid containing ≥90% of the cobalt precipitated from the product solutions. Thus Co_2O_3 or a related solid is produced when [Ru(III)] and [Co(II)] are

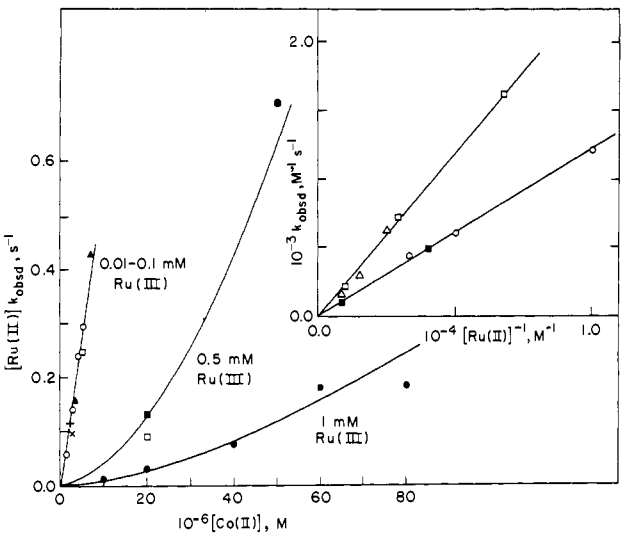

Figure 7. Behavior of the Co(II)-catalyzed system at pH 7.0, 25 °C. Upper right: the pseudo-second-order rate constant k_{obsd} as a function of $[Ru(bpy)_3^{2+}]^{-1}$ ((□) 1×10^{-4} M Ru(III), 5×10^{-6} M Co(II); (△) 3×10^{-4} M Ru(III), 2×10^{-5} M Co(II); (○) 3×10^{-5} M Ru(III), 2.8×10^{-6} M Co(II); (■) 5×10^{-4} M Ru(III), 2×10^{-5} M Co(II)). Lower left: the product of $[Ru(bpy)_3^{2+}]$ and k_{obsd} as a function of [Co(II)] ((●) 1×10^{-3} M Ru(III); (■) 5×10^{-4} M Ru(III); (+) 7×10^{-4} M Ru(III); (□) 1×10^{-4} M Ru(III); (▲) 5×10^{-5} M Ru(III); (○) 3×10^{-5} M Ru(III); (×) 1×10^{-5} M Ru(III)).

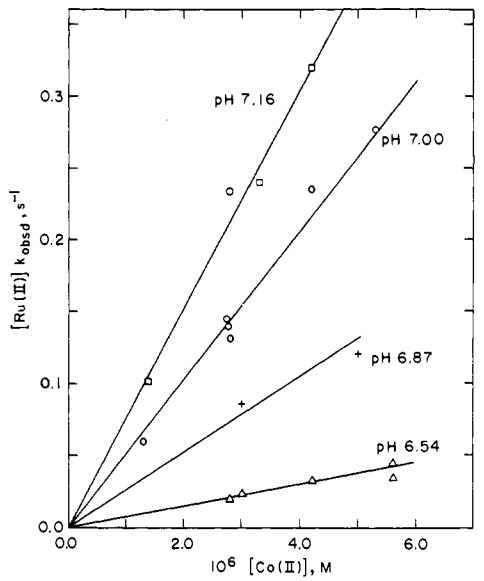

Figure 8. The pH dependence of the Co(II)-catalyzed reaction with 3.0×10^{-5} M initial $Ru(bpy)_3^{3+}$, $(1-3) \times 10^{-4}$ M $Ru(bpy)_3^{2+}$ added, 25 °C, and 0.1 M ionic strength: the product of $[Ru(bpy)_3^{2+}]$ and k_{obsd} as a function of [Co(II)] ((□) pH 7.16 ± 0.05; (○) pH 7.00 ± 0.05; (+) pH 6.87; (△) pH 6.54).

comparable and the O_2 yield is greatly diminished under these conditions.

Because of the complications described above, measurements were extended to lower Ru(III) and Co(II) concentrations. As can be seen in Figure 7, the rates exhibit a first-order dependence on [Co(II)] when $[Ru(III)]_0 \leq 1 \times 10^{-4}$ M. (Note that at very high [Ru(II)] the rates are Co(II) independent because of the rapidity of the noncatalyzed reaction, supplementary material, Table I.) The pH dependence of the rates in the range 6.5–7.2 was thus studied with 3.0×10^{-5} M $[Ru(III)]_0$. The results are summarized in Table IV and plotted in Figure 8. After the completion of the kinetic runs, the solutions were subjected to millipore filtration and their cobalt content was determined by atomic absorption: ≥90% of the cobalt originally added was present in the filtrate. In addition O_2 determinations (far right

Table IV. Rate Constants for the Co^{2+}-Catalyzed $Ru(bpy)_3^{3+}$–H_2O Reaction at 25 °C, 0.1 M Ionic Strength, in 0.025 M Phosphate Buffers[a]

10^5. $[Ru(III)]_0$, M	10^4. $[Ru(II)]_0$, M	10^6. [Co(II)], M	10^{-2}. k_{obsd}, M^{-1} s^{-1}	10^{-4}. $[Ru(II)]k_{obsd}/[Co(II)]$,[d] M^{-1} s^{-1}	yield[e] of O_2
		pH 7.0			
1.0	0.0	3.0			0.86
1.0	1.0	2.8	9.2	3.5	
3.0	0.0	3.0			0.81
3.0	1.0	2.8	12.1	4.6	0.66
3.0	2.0	2.8	6.1	4.6	
3.0	3.0	2.8	4.4	5.2	
3.0	3.0	1.3	1.9	4.6	0.40
3.0	3.0	4.2	7.5	5.6	
3.0	3.0	5.3	8.8	5.2	0.46
5.0	1.0	3.5	12.7[b]	4.5	
5.0	1.0	5.0			0.65
5.0	1.0	7.0	37.0[b]	6.7	
7.0	0.0	2.5	3.3[b]	4.6	
10.0	1.0	5.0	16.3	4.9	
10.0	3.0	5.0	7.2	5.0	
10.0	10.0	5.0	2.1	4.4	
		pH 6.54[c]			
3.0	0.0	3.0			0.83
3.0	1.0	2.8	1.98	0.79	0.59
3.0	1.0	5.6	3.87	0.79	
3.0	2.0	5.6	1.58	0.61	
3.0	1.0	4.2	3.30	0.94	
3.0	2.0	3.0	1.10	0.79	
		pH 6.87			
3.0	1.0	3.0	7.48	2.9	
3.0	2.0	5.0	5.59	2.6	
		pH 7.16			
3.0	0.0	3.0			0.96
3.0	2.0	2.8	10.9	7.9	
3.0	1.0	3.0			0.58
3.0	3.0	4.2	10.2	7.8	
3.0	1.0	1.4	8.86	7.3	
3.0	3.0	3.3	7.61	7.3	

[a] Argon-saturated solutions, ionic strength adjusted with Na_2SO_4, Ru(II) added as $Ru(bpy)_3Cl_2$. Unless otherwise stated, the reaction was monitored at 675 nm ($\epsilon_{Ru(III)}$ = 440 M^{-1} cm^{-1}) in a 10-cm cell. [b] Followed at 450 nm, $\Delta\epsilon = 1.4 \times 10^4$ M^{-1} cm^{-1}. [c] At this pH, the fits of the individual runs to a second-order Ru(III) dependence were poor, with curvature (reaction too slow) being significant after ~40% reaction. The k_{obsd} values reported were obtained from analysis of the first 40% reaction. [d] The [Ru(II)] used in this expression was the average Ru(II) during the run, i.e., $[Ru(II)]_0 + {}^1/_2[Ru(III)]_0 = [Ru(II)]$. [e] Yield based on eq 1; 22 °C, typically 0.5–1.0 μmol of O_2 produced.

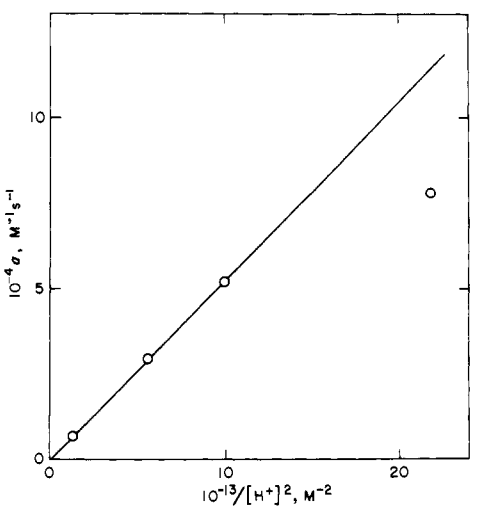

Figure 9. Slopes ($a = k_{obsd}[Ru(II)]/[Co(II)]$) from Figure 8 plotted as a function of $1/[H^+]^2$.

column of Table IV) confirmed that O_2 formation is near stoichiometric (eq 1) under these conditions. In Figure 9 the pH-dependent rate coefficients $k_{obsd}[Ru(II)]/[Co(II)]$ are plotted against $1/[H^+]^2$. It is evident that the rate coefficients are linear in $1/[H^+]^2$ between pH 6.5 and 7.0 but that the pH 7.16 point falls somewhat below the line of slope $k_{Co} = 5.3 \times 10^{-10}$ M s^{-1} drawn through the lower pH data points. The rate law in eq 7 is then deduced.

$$\frac{-d[Ru(III)]}{dt} = \frac{k_{Co}[Ru(III)]^2[Co(II)]}{[Ru(II)][H^+]^2} \quad (7)$$

Several runs were also undertaken with added H_2O_2 at the level which might be produced in the above runs if H_2O_2 is the precursor of O_2. The conditions used were 3×10^{-5} M $Ru(bpy)_3^{3+}$, 0.0 or 2×10^{-4} M Ru(II), 0.0 or 1×10^{-5} M H_2O_2, and pH 6.5 or 7.2 buffer. With added H_2O_2 neither Co(II) nor Ru(II) affected the rate of Ru(II) formation which was a least three times faster than that of the Co(II)-catalyzed runs (Table IV) at that pH. Analysis of the initial rates with added H_2O_2 in terms of the rate law[1] $-d[Ru(III)]/dt = k[H_2O_2][Ru(III)]$ gave $k = 430$ and 1820 M^{-1} s^{-1} at pH 6.5 and 7.16, respectively, in excellent agreement with the values calculated from the results reported in ref 1. In addition, with either H_2O_2 or Ru(III) in excess, stoichiometric O_2 was produced at pH 7 with $(0.03–1.0) \times 10^{-3}$ M Ru(III) (no added Co(II)).

Discussion

Mechanisms of the Thermal and Photochemical $Ru(bpy)_3^{3+}$-Reduction Processes. Spontaneous (i.e., noncatalyzed) reduction of $Ru(bpy)_3^{3+}$ in water is promoted by alkaline conditions, and at high pH a fairly simple dependence of the reduction rate on [Ru(III)] and $[OH^-]$ is found. There are at least five interpretations of this hydroxide dependence that need to be considered. (1) In order to account for *N*-oxide formation in the $Fe(bpy)_3^{3+}$ and $Fe(phen)_3^{3+}$ systems, Nord et al.[11] recently proposed rupture of the Fe^{III}–N(bpy) bond,[11] following OH^- attack on the nitrogen, as the rate-determining step for the Fe(III) systems. However, since neither free bpyO nor $Ru(bpy)_2(bpyO)^{2+}$ was detected as a product in this work, either different mechanisms operate in the Fe(III) and Ru(III) systems or the *N*-oxide found in the iron(III) system is produced in secondary reactions, for example, from free bpy or phen or through reactions of the partially dissociated species[11] (possibly intramolecular O-atom transfer in the $FeL_2O_2^{n+}$ species responsible for O_2 formation). (2) The second mechanism includes addition of OH^- to the ruthenium(III) center to give a seven-coordinate species followed by oxidation to give a ruthenyl (Ru(IV)) complex. In view of the very positive $E°$ for the Ru(IV)/Ru(III) couple,[19] a reaction producing Ru(IV) would be highly endergonic and would in all likelihood exhibit a second-order dependence on Ru(III) concentration. Such a dependence is not observed (in the absence of added cobalt(II)). (3) A third mechanism,[20] deprotonation of the 3-carbon in $Ru(bpy)_3^3$, was suggested recently by Serpone et al. Despite the fact that H–D exchange at the 3-carbon in $Ru(bpy)_3^{2+}$ does occur under rather forcing conditions,[21] no H–D exchanged species have been detected in the $Ru(bpy)_3^{3+}$ reaction products (present work) or in the $Fe(phen)_3^{3+}$ system.[10] (4) Earlier, rate-determining formation of free hydroxyl radical (and $M(bpy)_3^{2+}$) was proposed[9] but ruled out on the basis of energetic considerations. (Such a pathway, however, needs to be considered for extremely oxidizing species, e.g., $Ni(bpy)_3^{3+}$, $E° = 1.72$ V, particularly in light of the lower $\cdot OH/OH^-$ reduction potential, 1.89 V, recently obtained by Schwarz and Dodson.[22]) (5) The fifth mechanism,[1,10] which we continue to favor, involves nucleophilic addition of water or hydroxide to a bipyridine carbon in $M(bpy)_3^{3+}$. Hydroxide ion addition to activated aromatic amines finds precedent in the pseudobase formation reactions of both organic[23] and inorganic[20,24] species. As discussed below, such a mechanism can account for the products and rates obtained in the $Ru(bpy)_3^{3+}$ system. In addition this mechanism is consistent with the correlation of ML_3^{3+}/OH^- rate constant with $ML_3^{3+/2+}$ reduction potential (M = Fe, Ru, Os; L is a bpy or phen derivative) since for "isoelectronic" (low-spin d^5) 3+ metal centers the effective charge on the ligand might be expected to parallel the oxidizing power of the metal center.

In both thermal and photochemical processes ~0.9 mol $Ru(bpy)_3^{2+}$ and 0.02–0.2 mol CO_2 are produced per mol of $Ru(bpy)_3^{3+}$ taken. In addition, bpy-degraded ruthenium(II) complexes are formed. Reduction of $Ru(bpy)_3^{3+}$ is thus achieved at the expense of hydroxide ion or water-initiated oxidative degradation of a small fraction of the Ru(III). The equivalents for the reduction of $Ru(bpy)_3^{3+}$ are provided through the progressive degradation of a small number of coordinated bipyridines. One plausible pathway incorporating these features is shown in Scheme I.

Attack of water or hydroxide on the bipyridine ring yields a similar intermediate I_a in the thermal and light-induced reactions; in the latter case the nucleophilic addition involved in the formation of I_a is promoted by ligand-to-metal charge transfer (eq 8) while in the former case I_a is formed through intramolecular electron transfer in the initially formed Ru(III) pseudobase. Hydroxide/water attack may, of course, occur in parallel at several positions of the bipyridine ring, and the scheme is oversimplified in showing only 6/6′ attack. Since our observations do not establish the isomer distributions, we adopt this convention for the sake of simplicity. The same species I_a would also be obtained through hydroxyl radical attack on the 6/6′ position of $Ru(bpy)_3^{2+}$.[25] Pulse-radiolysis studies of the $Ru(bpy)_3^{2+}/OH·$[1] and $Fe(bpy)_3^{2+}/OH·$[26] reactions and the related $Fe(phen)_3^{2+}/OH·$,[27] phen/OH·,[27] and py/OH·[28] systems have elucidated some of the characteristics of "hydroxyl-radical adducts" such as I_a. They absorb strongly at long wavelengths[26–28] (as does the 750–800-nm-absorbing intermediate observed at neutral and high pH[1]) and are rapidly oxidized by outer-sphere oxidants such as $Fe(CN)_6^{3-}$ and $IrCl_6^{2-}$.[28] In the absence of added oxidants they dimerize or disproportionate to give the original N-heterocycle and a hydroxy-substituted derivative[27,28] while in the presence of a suitable oxidant they are converted stoichiometrically to an hydroxy-substituted N-aromatic,[28] their chemistry in this respect paralleling that of the aromatic hydrocarbons.[29] The oxidation of I_a by $Ru(bpy)_3^{3+}$ to give I_b is thus a reasonable step. The analogue of I_b has been isolated in the phen/OH· system,[27] and its pK_a is 8.1 for hydroxyl ionization. In the present system there is some evidence that side-product ***1*** corresponds to I_b (or an isomer).[30]

$$Ru^{III}(bpy)_3^{3+} \xrightarrow{h\nu} [Ru^{II}(bpy)_2(bpy^{+}\cdot)]^{3+} \quad (8)$$

(19) Gaudiello, J. G.; Bradley, P. G.; Norton, K. A.; Woodruff, W. H.; Bard, A. J. *Inorg. Chem.* **1984**, *23*, 3.
(20) Serpone, N.; Ponterini, G.; Jamieson, M. A.; Bolletta, F.; Maestri, M. *Coord. Chem. Rev.* **1983**, *50*, 209–302 and references cited therein.
(21) (a) Constable, E. C.; Seddon, K. R. *J. Chem. Soc., Chem. Commun.* **1982**, *34*. (b) McClanahan, S.; Hayes, T.; Kincaid, J. *J. Am. Chem. Soc.* **1983**, *105*, 4486.
(22) Schwarz, H. A.; Dodson, R. W., *J. Phys. Chem.*, in press.
(23) Bunting, J. W. *Adv. Heterocycl. Chem.* **1979**, *25*, 1.
(24) Gillard, R. D. *Coord. Chem. Rev.* **1975**, *16*, 67 and references cited therein.
(25) Supporting this assignment is the observation that **9** is produced in very high relative yield from the reaction of OH· and $Ru(bpy)_3^{2+}$ (work in progress); higher dimer yields are favored in the absence of oxidant (Ru(III)). The yield of ***7*** from the ·OH reaction is also large.
(26) Dimitrijević, N. M.; Mićić, O. I. *J. Chem. Soc., Dalton Trans.* **1982**, 1953.
(27) Floryan, E. S.; Pagsberg, P. *Int. J. Radiat. Chem.* **1976**, *8*, 425.
(28) Selvarajan, N.; Raghavan, N. V. *J. Phys. Chem.* **1980**, *84*, 2548.
(29) Walling, C. *Acc. Chem. Res.* **1975**, *8*, 125.
(30) The lack of pH dependence of the spectrum and $E_{1/2}$ of ***1*** appears surprising if ***1*** is indeed I_b, but similar results have also been obtained for the product of the $Fe(phen)_3^{2+}/OH·$ reaction.[27] Possibly the introduction of a single OH (or O^-) group does not alter the spectral and electrochemical properties detectably. Note that λ_{max} for $Fe(phen(O)_2)_3^{4-}$, the high pH form of the Fe(II) complex of 4,7-dihydroxyphenanthroline, is 520 nm, shifted only 10 nm from that of $Fe(phen)_3^{2+}$, λ_{max} 510 nm. (Schilt, A. A.; Smith, G. E.; Heimbuch, A. *Anal. Chem.* **1956**, *28*, 209.) Introduction of one rather than *six* OH/O^- groups is expected to result in even smaller spectral shifts.

Scheme I

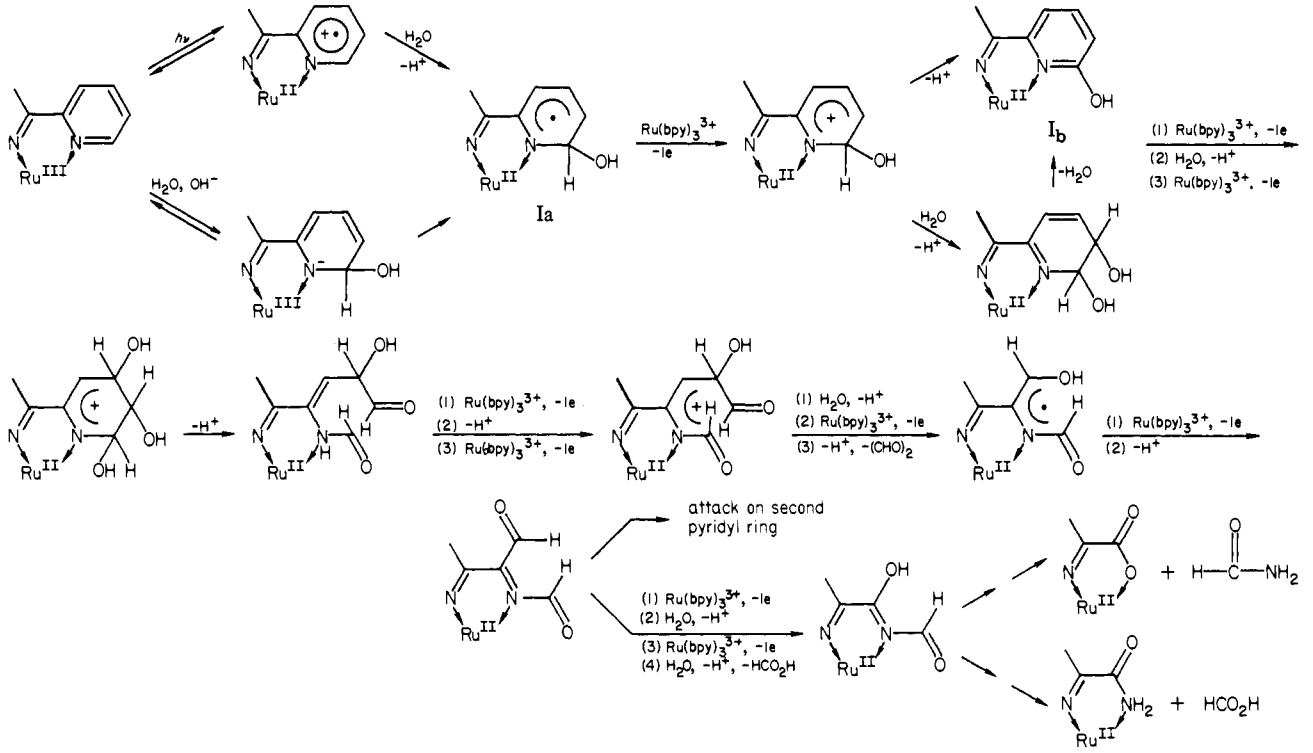

Above pH ~8 the hydroxyl group of I_b will be ionized, thus further promoting the susceptibility of the substituted bipyridine to oxidation. Subsequent oxidations commencing with the "hydroxypyridine"[28] I_b or its hydrate *could* proceed as in Scheme I, but the sequence is intended only to show how CO_2 and different Ru(II) complexes may arise; our observations do not establish the detailed oxidation sequence. In terms of the proposed scheme the CO_2 results either from oxidation of formate or from direct decarboxylation of intermediates analogous to those shown. While degradation of only one of the pyridines is illustrated, more than one ring may be attacked. In addition, the radical intermediates shown in Scheme I could dimerize to yield higher charged complexes: the strongly retained compounds ***8*** and ***9*** (Figure 1) probably correspond to such dimeric substances.[25,31]

The origin of the chemiluminescence is a matter of some interest. Reduction of $Ru(bpy)_3^{3+}$ to $*Ru(bpy)_3^{2+}$ occurs in high yield with a number of strong reductants,[32] e.g., e_{aq}^-, $Ru(bpy)_3^+$, $CO_2^{-\cdot}$. In these systems a simple outer-sphere electron-transfer pathway is likely, and the excited state is formed at the expense of ground-state $Ru(bpy)_3^{2+}$, presumably because the reaction leading to the latter product is extremely exergonic (lies in the inverted region). Chemiluminescence for more complex reductants[33] such as hydrazine,[17] EDTA, BH_4^-, etc. likely involves the reaction of intermediate radical species with $Ru(bpy)_3^{3+}$—rather than the reaction of the formal reductant. The $Ru(bpy)_3^{3+}/OH^-$ reaction also falls into this category since simple reaction of $Ru(bpy)_3^{3+}$ and OH^- (to produce $*Ru(bpy)_3^{2+}$ + ·OH) is endergonic by nearly 3 eV. The complexity of the chemiluminescent–time profiles confirms a complicated mechanism for excited-state production. It is chemically reasonable that reaction of $Ru(bpy)_3^{3+}$ with one (or more) of the highly reducing ($E° < -0.84$ V) radical species, such as those shown in Scheme I, produces $*Ru(bpy)_3^{2+}$.

Scheme II

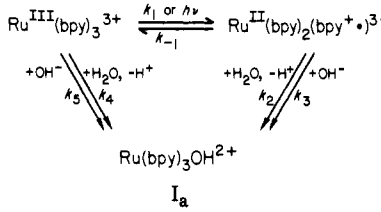

followed by

$$Ru(bpy)_3OH^{2+} + (n-1)Ru(bpy)_3^{3+} \rightarrow \text{products}$$

We now consider the rate law for Ru(III) reduction. Earlier[1] we proposed Scheme II, which gives eq 9

$$\frac{-d[Ru(III)]}{[Ru(III)dt} = n\left\{\left[\frac{k_2 + k_3[OH^-]}{k_{-1} + k_2 + k_3[OH^-]}\right]k_1 + k_4 + k_5[OH^-]\right\} \quad (9)$$

as the rate expression when the steady-state approximation is applied to the concentrations of the various intermediates. The intermediate $[Ru^{II}(bpy)_2(bpy^+)]^{3+}$ can now be identified with the LMCT excited state of $Ru(bpy)_3^{3+}$, and our recent work permits evaluation of k_1, k_{-1}, and k_2 and the relevance of this intermediate to the dark reaction kinetics.

The lifetime of $*Ru(bpy)_3^{3+}$ ($\equiv Ru^{II}(bpy)_2(bpy^+)^{3+}$) is ~3 × 10^{-12} s in 9 M H_2SO_4 at 25 °C,[34] and thus the nonradiative decay rate constant $k_{-1} \sim 3 \times 10^{11}$ s^{-1}. The quantum yield for $Ru(bpy)_3^{3+}$ disappearance in 1 M H_2SO_4, 2×10^{-4}, is given by

$$\phi = \frac{n(k_2 + k_3[OH^-])}{k_{-1} + k_2 + k_3[OH^-]}$$

where n is the number of $Ru(bpy)_3^{3+}$ molecules consumed per excited state reacting. Since $\phi \ll 1$ the above equation reduces to $\phi = n(k_2 + k_3[OH^-])/k_{-1}$ from which $n(k_2 + k_3[OH^-]) \sim 6 \times 10^7$ s^{-1}. Since k_3 cannot exceed ~10^{11} M^{-1} s^{-1}, $k_3[OH^-] < 10^{-3}$ s^{-1}, only k_2 is relevant to the 1 M acid experiments and $nk_2 \sim$

(31) Interestingly, recent experiments with colloidal TiO_2 have demonstrated the photooxidation of benzoic acid via intermediate formation of salicylic acid (Izumi, I.; Fan, F. F.; Bard, A. J. *J. Phys. Chem.* **1981**, *85*, 218), and the photooxidation of toluene to form cresols (Fujihira, M.; Satoh, Y.; Osa, T. *Nature (London)* **1981**, *293*, 206).

(32) Balzani, V.; Boletta, F. *Comments Inorg. Chem.* **1983**, *2*, 211. Tokel-Takvoryan, N. E.; Hemingway, R. E.; Bard, A. J. *J. Am. Chem. Soc.* **1973**, *95*, 6582.

(33) Gafney, H. D.; Adamson, A. W. *J. Chem. Educ.* **1972**, *52*, 481.

(34) Bergkamp, M.; Gütlich, P.; Netzel, T.; Sutin, N. *J. Phys. Chem.* **1983**, *87*, 3877.

6×10^7 s^{-1}. Even if n is as large as 10, k_2 is 10^6 s^{-1} or greater. Thus, despite the small quantum yield, the reaction of $*Ru(bpy)_3^{3+}$ with water is an extremely rapid reaction. Similar observations have been made for $Fe(phen)_3^{3+}$ LMCT irradiation.[35,36] The low quantum yields observed in these systems are due, to a large extent, to the very short lifetimes ($<10^{-11}$ s at room temperature) of the LMCT excited states. The role of water in determining both the dark and photoreduction rates is also noteworthy: the photoreduction of $Fe(phen)_3^{3+}$ occurs with detectable yield only in the presence of water—the quantum yield is essentially zero in 98% sulfuric acid.

The relevance of the thermally populated excited-state pathway to the dark reaction kinetics (first term in eq 9) depends upon the magnitude of k_1/k_{-1} since $k_{-1} \ll k_2 + k_3[OH^-]$ below pH ~14. The value of k_1/k_{-1} is determined by E^* for the formation of $*Ru(bpy)_3^{3+}$ (eq 10). From the absorption spectrum of $Ru(bpy)_3^{3+}$ (λ_{max} 675 nm) $E^* \leq 1.8$ eV, while the recent electrochemical results of Gaudiello et al.[19,37] implicate $*E \sim 1.76$ eV. Thus k_1/k_{-1} is estimated as 10^{-30}, k_1 as 4.4×10^{-19} s^{-1}, and nk_1k_2/k_{-1}, the dark reaction rate constant in acid via this path, as 6×10^{-23} s^{-1}. Since the measured rate constant exceeds this value (and k_1) by many orders of magnitude, it is concluded that the excited-state pathway does not contribute to the dark reaction rates.

$$Ru(bpy)_3^{3+} \rightleftharpoons *Ru(bpy)_3^{3+} \qquad E^* \qquad (10)$$

The above result suggests re-interpretation of the intermediate-pH kinetic data. As noted earlier,[1] the observed kinetics for buffered pH 7–10 solutions depend upon the initial $Ru(bpy)_3^{3+}$ concentration and the solution pH, and the measured rates are more rapid than would be predicted from the rate law measured at extreme pH. When Scheme II and eq 9 were originally proposed, the extent of $Ru(bpy)_3^{3+}$ degradation was not fully appreciated and the stoichiometric factor n was taken as 2. From the present work (see Table I and Scheme I), it is evident that n may be on the order of 10. In addition, since water/hydroxide addition and oxidation of the resulting intermediates compete for $Ru(bpy)_3^{3+}$ and since the fate of the intermediates may be pH dependent (note the variable side-product distribution in Table I), n is likely to be a function of the conditions used. This variability of the stoichiometric factor is most likely the source of the [Ru(III)] dependence of the pH 7–10 kinetics and the apparently too rapid rates found at intermediate pH could simply reflect stoichiometry changes. The observed kinetics in buffered solutions are then attributed to attack of OH^- or water on $Ru(bpy)_3^{3+}$ (with rate constants nk_5 and nk_4, respectively), and the species $(bpy)_2Ru(bpy^+)^{3+}$ in Scheme II is important in the photochemical reaction alone. Thus eq 9 can be simplified to

$$\frac{-d[Ru(III)]}{[Ru(III)]dt} = n\{k_4 + k_5[OH^-]\} \qquad (11)$$

which reduces to eq 6 when $k_5[OH^-] \gg k_4$.[38]

Scheme III

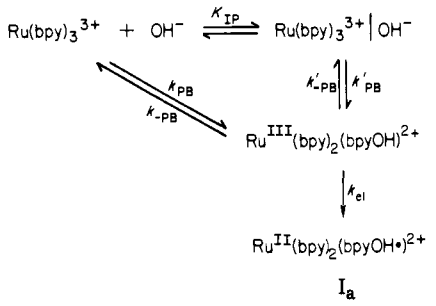

The detailed parameters for the thermal and photochemical paths may now be compared. Neglecting differences in the stoichiometric factors, and assuming the reaction of $*Ru(bpy)_3^{3+}$ to be diffusion limited, the reaction of excited $Ru(bpy)_3^{3+}$ with hydroxide ion is 10^9 ($k_3/k_5 = 10^{11}/10^2$) times more rapid than the ground-state reaction and the reaction with water is 10^{12} ($k_2/k_4 = 6 \times 10^7/10^{-5}$) more rapid for the excited state. Thus excitation of $Ru(bpy)_3^{3+}$ results in a striking reactivity enhancement which is of the magnitude expected on the basis of the driving force differences ($k^*/k \sim \exp(E^*/2RT)$) for the excited- and ground-state reactions.

Having ruled out any contribution of the excited-state pathway to the dark reaction kinetics, we return to the pseudobase mechanism for the formation of I_a, specifically the detailed pathway for k_5 in Scheme II. This is elaborated in Scheme III. Nucleophilic addition of hydroxide ion to bpy carbon in $Ru(bpy)_3^{3+}$ (possibly via the ion pair ($K_{IP} \sim 1$ M^{-1} [39])) yields the transient Ru(III) pseudobase ($K_{PB} = k_{PB}/k_{-PB} < 1$ M^{-1} [40]) which undergoes intramolecular electron transfer to give the Ru(II) radical I_a. Conversion of the pseudobase to I_a is assumed quantitative because the reverse reaction (conversion of $Ru(bpy)_3^{2+}$–hydroxyl radical adduct to Ru(III)) is not observed.[1] If this intramolecular electron transfer (k_{el}) is also assumed to be rapid compared to OH^- loss from the pseudobase ($k_{el} \gg k_{-PB}, k'_{-PB}$), then k_5 is equal to the rate constant for pseudobase formation. If the ion-pair pathway is neglected for the sake of simplicity and the fact that n $Ru(bpy)_3^{3+}$ are consumed per pseudobase formed is taken into account, then $k_a = nk_{PB} = 1.5 \times 10^2$ M^{-1} s^{-1}. From the product studies n is 5–20 and so k_{PB} is of the order of 10^1 M^{-1} s^{-1}, a value which is not unreasonable in light of those found in other systems.[41] Analogously, the rate constant $\sim 10^{-5}$ s^{-1} determined for $Ru(bpy)_3^{3+}$ reduction in very acid media may be ascribed to pseudobase formation via nucleophilic addition of water to the bound bipyridine ring. Neglecting differences in stoichiometric factors in acid and base, the ratio k_{OH}/k_{H_2O} for pseudobase formation is calculated to be $\sim 10^9$. The ratio 10^7 has been found for a number of organic pseudobase systems.[23]

Mechanism of the Co(II) Catalysis of the Oxidation of Water by $Ru(bpy)_3^{3+}$. Aquocobalt(II) catalyzes water oxidation to O_2 for a number of powerful one-electron oxidizing agents[3] including $Fe(bpy)_3^{3+}$ and $IrCl_6^{3-}$ in addition to the $Ru(bpy)_3^{3+}$ system under consideration. Cobalt(IV) has been proposed as the active catalyst in such systems[3] although only the $Ru(bpy)_3^{3+}$ system has been subjected to a detailed kinetics investigation.[4] It will be recalled that at low Ru(III) to Co(II) ratios and low [Co(II)] the rate law for $Ru(bpy)_3^{3+}$ consumption is given by

$$\frac{-d[Ru(III)]}{dt} = \frac{k_{Co}[Ru(III)]^2[Co(II)]}{[Ru(III)][H^+]^2} \qquad (7)$$

(35) Wehry, R. L.; Ward, R. A. *Inorg. Chem.* **1971**, *10*, 2660.
(36) Malik, G. H.; Laurence, G. S. *Inorg. Chim. Acta* **1978**, *28*, L149.
(37) Gaudiello, J. G.; Sharp, P. R.; Bard, A. J. *J. Am. Chem. Soc.* **1982**, *104*, 6373.
(38) It is difficult to simultaneously fit the chemiluminescence time dependences and yields. The following scheme will give rise to the behavior found at "high" Ru(III) and [OH^-] (Figure 3):

$$Ru(bpy)_3^{3+} + OH^- \rightarrow I_a \xrightarrow{Ru(III),\ OH^-} P_i + Ru(III) \qquad (1)$$

$$Ru(bpy)_3^{3+} + OH^- \rightarrow I_a' \qquad (2)$$

$$I_a' + Ru(III) \rightarrow I_b' \qquad (3)$$

$$I_b' + Ru(III) \rightarrow *Ru(bpy)_3^{2+} \qquad (4)$$

$$I_b' + P_i \rightarrow *Ru(bpy)_3^{2+} \qquad (5)$$

Here eq 1 summarizes "the" main reaction path (Schemes I and II) and eq 2 involves a minor reaction pathway, perhaps attack of OH^- at the 3- or 4-carbon in bipyridine. In eq 3 oxidation of I_a' (analogous to I_a) to I_b' (analogous to I_b) is invoked. The time and yield data can be modelled if I_b' reacts with both Ru(III) (eq 4) and a product or products (P_i, eq 5) of the main sequence (i.e., $\{k_4[Ru(III)]_t + k_5[P_i]_t\} \propto [Ru(III)]_0$) to give the excited state responsible for the chemiluminescence.

(39) The $Ru(bpy)_3^{3+}/OH^-$ ion pair constant is estimated as 1.7 and 0.9 M^{-1} at 0.1 and 1 M ionic strength, respectively, from the usual expressions.
(40) For alkyl N-substituted phenanthrolines $K_{PB} = 10^4$–10^5 M^{-1} (Bunting, J. W.; Meathrel, W. G. *Can. J. Chem.* **1974**, *52*, 975). The fact that the spectrum of $Rh(bpy)_3^{3+}$ is the same in acid and 2 M NaOH suggests $K_{PB} \ll 1$ M^{-1} for this 3+ metal complex. For $Ru(bpy)_3^{3+}$ K_{PB} might be expected to be somewhat larger than for $Rh(bpy)_3^{3+}$ but substantially smaller than for the N-alkyl dications.
(41) For example, for $Ru(5\text{-}(NO_2)phen)_3^{2+}$ $K_{PB} = 32$ M^{-1} and $k_{PB} = 1.8$ M^{-1} s^{-1}.[24]

As $[Ru(bpy)_3^{3+}]$ is increased from $\leq 1 \times 10^{-4}$ M to $\geq 5 \times 10^{-4}$ M, $[Co(II)] \sim 10^{-5}$ M, the form of the rate law is the same but k_{Co} diminishes. In addition, when [Co(II)] and [Ru(III)] are comparable no O_2 is formed. These observations do indeed implicate Co(IV) with a scheme such as eq 12–15 and 17 as part of the catalytic sequence, and eq 16 to account for catalyst loss.

$$Co^{2+} + 2H_2O \overset{K_{12}}{\rightleftharpoons} Co(OH)_2 + 2H^+ \quad (12)$$

$$Co(OH)_2 + Ru(III) \underset{k_{-13}}{\overset{k_{13}}{\rightleftharpoons}} Co(OH)_2^+ + Ru(II) \quad (13)$$

$$Co(OH)_2^+ + Ru(III) \xrightarrow[k_{14}]{slow} CoO^{2+} + Ru(II) + H_2O \quad (14)$$

$$CoO^{2+} \xrightarrow[H_2O]{k_{15}} Co^{2+} + H_2O_2 \quad (15)$$

$$CoO^{2+} + Co(II) \xrightarrow{k_{16}} CoOCo^{4+} \rightarrow "Co_2O_3"_s \quad (16)$$

$$2Ru(III) + H_2O_2 \rightarrow 2Ru(II) + O_2 + 2H^+ \quad (17)$$

The Co(II), Ru(III), and Ru(II) dependence in eq 7 implicates eq 14, formation of Co(IV) via oxidation of Co(III) species by $Ru(bpy)_3^{3+}$, as the rate-determining step.[42] The Co(III) species, written as $Co(OH)_2^+$ to accord with the $1/[H]^2$ dependence of the rate, is formed through the pre-equilibria eq 12 and 13. Oxidation of hydrolyzed Co(II) ($K_{12} \sim 2.2 \times 10^{-10}$ M^2 [43]) produces Co(III) (eq 13). From the $Co(H_2O)_6^{3+/2+}$ reduction potential (1.86 V[44]) and estimated Co(II) and Co(III) hydrolysis constants,[43] the $E°$ for the $Co(OH)_2^{+/0}$ couple is ~1.1 V. The overall pre-equilibrium forming cobalt(III) then lies to the left in neutral solution; i.e., at pH 7, $K_{12}K_{13}/[H^+]^2 \sim 10^{-2}$ ($E°$ $Ru(bpy)_3^{3+/2+} = 1.26$ V). The breakdown in the $1/[H^+]^2$ dependence (see Figure 9) at pH 7.2 may be due to further hydrolysis of Co(III) to give species that are less rapidly oxidized by Ru(III). Provided that Co^{2+} and $Co(OH)_2^+$ are the dominant forms of Co(II) and Co(III), respectively (where complexing by phosphate is not excluded), k_{Co} is equal to $nK_{12}K_{13}k_{14}$ where n is 4 when reaction 17 is sufficiently rapid (as was confirmed by our studies with added H_2O_2). Substitution for the various parameters gives $k_{14} \sim 1 \times 10^6$ M^{-1} s^{-1} and $k_{15} \geq 100$ s^{-1}. In addition, successful simulations of the time profiles at high Ru(III) (where eq 16 predominates) yield $k_{16} \sim 10^4 k_{15}$ M^{-1} $\geq 10^6$ M^{-1} s^{-1}, compatible with substitution on aquocobalt(II). Interestingly, eq 7 and these parameters also correctly predict rates ($\sim 10^{-8}$ M s^{-1} of O_2) found in the pH 5 photochemical experiments described by Harriman et al.[45]

The Co(IV) product in eq 14 is written as the "yl" CoO^{2+} by analogy with other M(IV) species. Reaction of CoO^{2+} with water (or hydroxide) gives H_2O_2 and Co(II); production of peroxide is chemically reasonable, especially in light of electrochemical studies of Co(II).[46] Oxidation of H_2O_2 by $Ru(bpy)_3^{3+}$ (eq 17) completes the O_2 formation sequence, while eq 15 regenerates the catalyst. The net reaction, Ru(II) formation and Co(III) precipitation, found when [Ru(III)] and [Co(II)] are equal, results from eq 12–14 and 16 (or eq 12, 13, and 18). The diminished catalyst

$$2Co(OH)_2^+ \rightarrow Co_2O_3 + H_2O + 2H^+ \quad (18)$$

activity at high Ru(III) is also ascribed to eq 16; this reaction converts part of the Co(IV) and Co(II) to an inactive Co(III) species each cycle and is written by analogy with the behavior of other yl ions.[47] At high [Co(II)] and high [Ru(III)]/[Co(II)] ratios, the effective catalyst concentration is thereby diminished by the formation of inactive hydrolyzed cobalt(III) species.

The proposed mechanism for Co(II) catalysis of water oxidation to O_2 accounts satisfactorily for rates and product distributions in the $Ru(bpy)_3^{3+}$ system. In addition, it provides a general mechanism which may apply for the other systems in which Co(II) catalysis of oxygen formation has been found. In general, the catalysis probably proceeds through outer-sphere one-electron oxidations to produce Co(IV). Depending on the pH and the nature of the oxidant, different steps in the sequence may, of course, become rate determining. For example, with oxidants stronger than $Ru(bpy)_3^{3+}$ or for $Ru(bpy)_3^{3+}$ at higher pH, eq 15, peroxide formation, could become rate limiting. Unfortunately cobalt hydrolysis (for all three oxidation states) and phosphate complexing introduce complexities which may obscure the genuine mechanistic features under some conditions: the Co(II) dependence of the O_2 yields (Figure 5), maximizing at [Ru(III)]/[Co(II)] ~ 10 at pH 7 and [Ru(III)]/[Co(II)] ~ 100 at pH 9, is a case in point since this Co(II) dependence most likely arises through loss of active catalyst (and Ru(III)) to hydrolyzed insoluble (inactive) Co(III) at high initial [Co(II)].

Finally, it is worth contrasting the role of the ruthenium complex in this system with the roles of ruthenium complexes in the $[Ru(bpy)_2(H_2O)]_2O^{4+}$ [5] and $RuL_2py(H_2O)^{2+}$ (L = 2-phenylazopyridine)[6] systems also recently reported to effect water oxidation. In the latter, Ru(IV) or even higher oxidation states fulfill the role of Co(IV) (site for O–O bond formation) in the present system. By contrast, the role of $Ru(bpy)_3^{3+}$ in the presence of Co(II) is to provide the oxidizing equivalents for Co(IV) formation. The formation of a highly oxidizing yl ion (CoO^{2+}, RuL_2pyO^{2+},[6] etc.) thus appears to be a feature common to the homogeneous catalysts presently known. The details of the reactions of these active yl ions with water remain to be characterized.

Conclusions

In the absence of added catalysts the water/hydroxide-induced reduction of $Ru(bpy)_3^{3+}$ yields $Ru(bpy)_3^{2+}$, bpy oxidation products including CO_2, and Ru(II) complexes containing bpy and oxidized bpy. The rate of $Ru(bpy)_3^{3+}$ reduction is pH dependent; k_{obsd} values at 25 °C increase from 10^{-5} s^{-1} in 1 M H_2SO_4 to $\sim 10^{-3}$ s^{-1} at pH 7 to 150[OH$^-$] s^{-1} above pH 12. This pH dependence and the products obtained are ascribed to rate-determining attack of hydroxide (water) on bpy-carbon to give a transient pseudobase. Subsequent oxidation of this OH$^-$ adduct and its oxidation products consumes ~10 $Ru(bpy)_3^{3+}$ and yields CO_2 and a pH-dependent distribution of ring-oxidized Ru(II) complexes.

At pH >7, the presence of catalytic Co(II) ([Co(II)] ~ 0.1-[Ru(III)]) promotes stoichiometric oxidation of water by $Ru(bpy)_3^{3+}$. On the basis of rate and product studies, a catalysis mechanism involving rate-determining production of Co(IV) (from Co(III) formed in a rapid-preequilibrium reaction of Co(II) and Ru(III)) is implicated. The Co(IV) reacts with water to give H_2O_2 and regenerate Co(II) but may be diverted by Co(II) to give an inactive Co(III) polymer with consequent loss of catalytic activity. In addition when [Co(II)] and [Ru(III)] are comparable Co_2O_3 is formed at the expense of O_2.

Both degradative and Co(II)-catalyzed reaction paths appear to derive largely from the high-oxidation potential of the $Ru(bpy)_3^{3+/2+}$ couple. In the first case, the charge on the metal is responsible for activation of the ligand toward OH$^-$ addition. The subsequent bpy oxidation steps consume $Ru(bpy)_3^{3+}$ probably through a series of one-electron outer-sphere reactions. Similarly in the Co(II)-catalyzed path the role of $Ru(bpy)_3^{3+}$ is largely to

(42) Note that this mechanism is not unique. The following (and variants) are also consistent with the observed rate law:

$$2Ru(III) \rightleftharpoons Ru(IV) + Ru(II)$$

$$Ru(IV) + Co(OH)_2 \rightarrow Ru(II) + Co(IV) \text{ etc.}$$

This interpretation seems less attractive than the scheme considered because of the very positive $E°$ for the Ru(IV)/Ru(III) couple. See ref 19 and 37. In addition, since Co(II) catalyzes water oxidation by a wide variety of one-electron oxidants including $IrCl_6^{2-}$ [3] and $Ni(bpy)_3^{3+}$ (Chan, S.-F., work in progress), a sequence based on sequential one-electron oxidations of Co^{n+} is more attractive.

(43) Baes, C. F., Jr.; Mesmer, R. E. "The Hydrolysis of Cations"; Wiley-Interscience: New York, 1976, p 238. K_{nh} is defined as the equilibrium constant for $M^+ + nH_2O \rightleftharpoons M(OH)_n^{(1-n)+} + nH^+$. The following log K_{nh} values were used here: Co(II) −9.65 (n = 1), −18.8 (n = 2); Co(III) −2.5 (n = 1), −5.9 (n = 2). The Fe(III) values (p 230) were used for Co(III).

(44) Warnquist, B. *Inorg. Chem.* **1970**, *9*, 682.

(45) Harriman, A.; Porter, G.; Walters, P. *J. Chem. Soc., Faraday Trans.* **1981**, *2*, 2373.

(46) Shafirovich, V. Ya.; Strelets, V. V. *Nouv. J. Chim.* **1978**, *2*, 199 footnote 10.

(47) (a) Newton, T. W.; Baker, F. B. *Inorg. Chem.* **1964**, *3*, 569. (b) Conochiolli, T. J.; Hamilton, E. J., Jr.; Sutin, N. *J. Am. Chem. Soc.* **1965**, *87*, 926.

supply oxidizing equivalents to generate Co(IV) on which the O–O bond is assembled. In these reactions the role of Ru(III) is in contrast to recently described systems in which Ru(II)/(IV) couples, etc. effect inner-sphere water oxidation.

Acknowledgment. We are indebted to Drs. Mark A. Andrews and Tony Chang, who made the IR and NMR measurements and whose comments have been extremely helpful. We also thank Ms. Elinor Norton, who performed analyses for ruthenium. This work was performed at Brookhaven National Laboratory under contract with the U.S. Department of Energy and supported by its Office of Basic Energy Sciences.

Registry No. $Ru(bpy)_2(bpyO)^{2+}$, 90912-91-7; $Ru(bpy)_3^{3+}$, 18955-01-6; Co, 7440-48-4; H_2O, 7732-18-5.

Supplementary Material Available: Method for chemiluminescence yield calibration and rate constants for $Ru(bpy)_3^{3+}$ reduction at pH 7 as a function of Ru(III) and Ru(II) concentrations (5 pages). Ordering information is given on any current masthead page.

Trinuclear Osmium Clusters as Models for Intermediates in CO Reduction Chemistry. 2. Conversion of a Methylene into a Ketene Ligand on a Triosmium Cluster Face

Eric D. Morrison,[1a] Guy R. Steinmetz,[1a] Gregory L. Geoffroy,*[1a] William C. Fultz,[1b] and Arnold L. Rheingold[1b]

Contribution from the Departments of Chemistry, The Pennsylvania State University, University Park, Pennsylvania 16802, and the University of Delaware, Newark, Delaware 19711.
Received November 25, 1983

Abstract: The bridging methylene complex $Os_3(CO)_{11}(\mu\text{-}CH_2)$ (**3**) reacts with CO to give the new ketene complex $Os_3(CO)_{12}(\eta^2\text{-}(C,C),\mu_2\text{-}CH_2CO)$ (**4**) in high yield. Complex **4** has been spectroscopically as well as structurally characterized. It crystallizes in the space group $P2_1/n$, with $a = 9.414$ (2) Å, $b = 15.369$ (3) Å, $c = 13.940$ (4) Å, $\beta = 107.9$ (2)°, $V = 1918.6$ (7) Å,[3] and $Z = 4$. Least-squares refinement of the 3015 reflections with $(F_o)^2 > 3\sigma(F_o)^2$ converged to $R = 0.033$ and $R_w = 0.034$. The ketene ligand is incorporated into a triosmacyclopentanone ring and bridges between two Os atoms that are not joined by a metal–metal bond. Bond angles imply sp^3 and sp^2 hybridization for the CH_2 and CO carbon atoms, respectively. Complex **4** reacts with H_2O and CH_3OH to yield CH_3COOH and CH_3COOCH_3, respectively, along with $Os_3(CO)_{12}$. Reaction of **4** with H_2 yields CH_3CHO and the clusters $H_2Os_3(CO)_{10}$ and $H_4Os_4(CO)_{12}$. The formation of **4** can be partially reversed to **3** by heating in vacuo, although the thermal instability and moisture sensitivity of **4** preclude quantitative recovery of $Os_3(CO)_{11}(\mu\text{-}CH_2)$. Carbon-13 labeling experiments show that the ketene carbonyl derives from one of the original cluster carbonyls rather than from the added CO. The possible relevance of the $\mu\text{-}CH_2 \rightarrow \mu\text{-}CH_2CO$ conversion to the mechanism of formation of C_2-oxygenated products during CO reduction catalysis is discussed.

A large number of methylene-bridged transition-metal compounds have been prepared, and their chemistry is under active investigation.[2] However, one important reaction that has not been well-documented for this class of compounds is the insertion of CO into a metal–methylene bond to yield a coordinated ketene, eq 1. Such reaction may be of relevance to the mechanism for

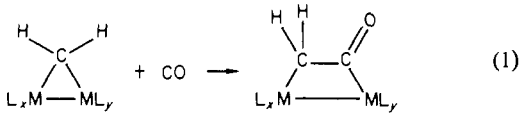

(1)

chain growth during CO reduction over heterogeneous catalysts where surface-bound methylene ligands are believed important.[3] In particular, the CO insertion into a metal–methylene bond to give a surface ketene ligand could be an important step in the formation of C_2-oxygenated products. Such reaction has been suggested by Ichikawa et al.[4a] to play an important role in the high-yield formation of ethanol from CO/H_2 over certain $Rh/ZrO_2/SiO_2$ and $Rh/TiO_2/SiO_2$ catalysts, eq 2. Recent isotopic

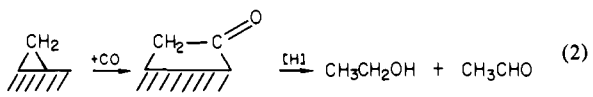

(2)

tracer experiments on ethanol synthesis from CO/H_2 by Takeuchi and Katzer[4b] also indicate that this product forms via CO insertion into a surface-methylene bond as indicated in eq 2.

A few mononuclear carbene complexes have been shown to insert or add CO to give complexes containing ketene ligands.[5] Only recently has evidence been obtained for similar reactions with polynuclear μ-carbene complexes. Curtis and Messerle[6] observed $Ph_2C{=}C{=}O$ as a product from the reaction of $Cp_2Mo_2(CO)_4(\mu\text{-}CPh_2)$ with CO, a reaction which may proceed via a bridging diphenylketene complex. Keim et al.[7] have noted that $Fe_2(CO)_8(\mu\text{-}CH_2)$ reacts with methanol and ethanol in the presence of CO to yield the corresponding acetates and presented evidence that these reactions proceed through the unstable bridging ketene complex **1**, eq 3. Lin et al.[8] recently reported insertion

(1) (a) The Pennsylvania State University. (b) The University of Delaware.
(2) For a recent review see: Herrmann, W. A. *Adv. Organomet. Chem.* **1982**, *20*, 159.
(3) (a) Muetterties, E. L.; Stein, J. *Chem. Rev.*, **1979**, *79*, 479. (b) Bell, A. T. *Catal. Rev.* **1981**, *23*, 203. (c) Herrmann, W. A. *Angew. Chem., Int. Ed. Engl.* **1982**, *21*, 117. (d) Pettit, R.; Brady, R. C., III *J. Am. Chem. Soc.* **1980**, *102*, 6181. (e) Pettit, R.; Brady, R. C., III *Ibid.* **1981**, *103*, 1287.
(4) (a) Ichikawa, M.; Sekizawa, K.; Shikakura, K.; Kawai, M., *J. Mol. Catal.* **1981**, *11*, 167. (b) Takeuchi, A.; Katzer, J. R. *J. Phys. Chem.* **1982**, *86*, 2438.
(5) (a) Herrmann, W. A.; Plank, J. *Angew. Chem., Int. Ed. Engl.* **1978**, *17*, 525. (b) Cutler, A. R.; Bodner, T. *J. Am. Chem. Soc.* **1983**, *105*, 5926.
(6) Messerle, L.; Curtis, M. D. *J. Am. Chem. Soc.* **1980**, *102*, 7789.
(7) Röper, M.; Strutz, H.; Keim, W. *J. Organomet. Chem.* **1981**, *219*, C5.
(8) Lin, Y. C.; Calabrese, J. C.; Wreford, S. S. *J. Am. Chem. Soc.* **1983**, *105*, 1679.

0002-7863/84/1506-4783$01.50/0